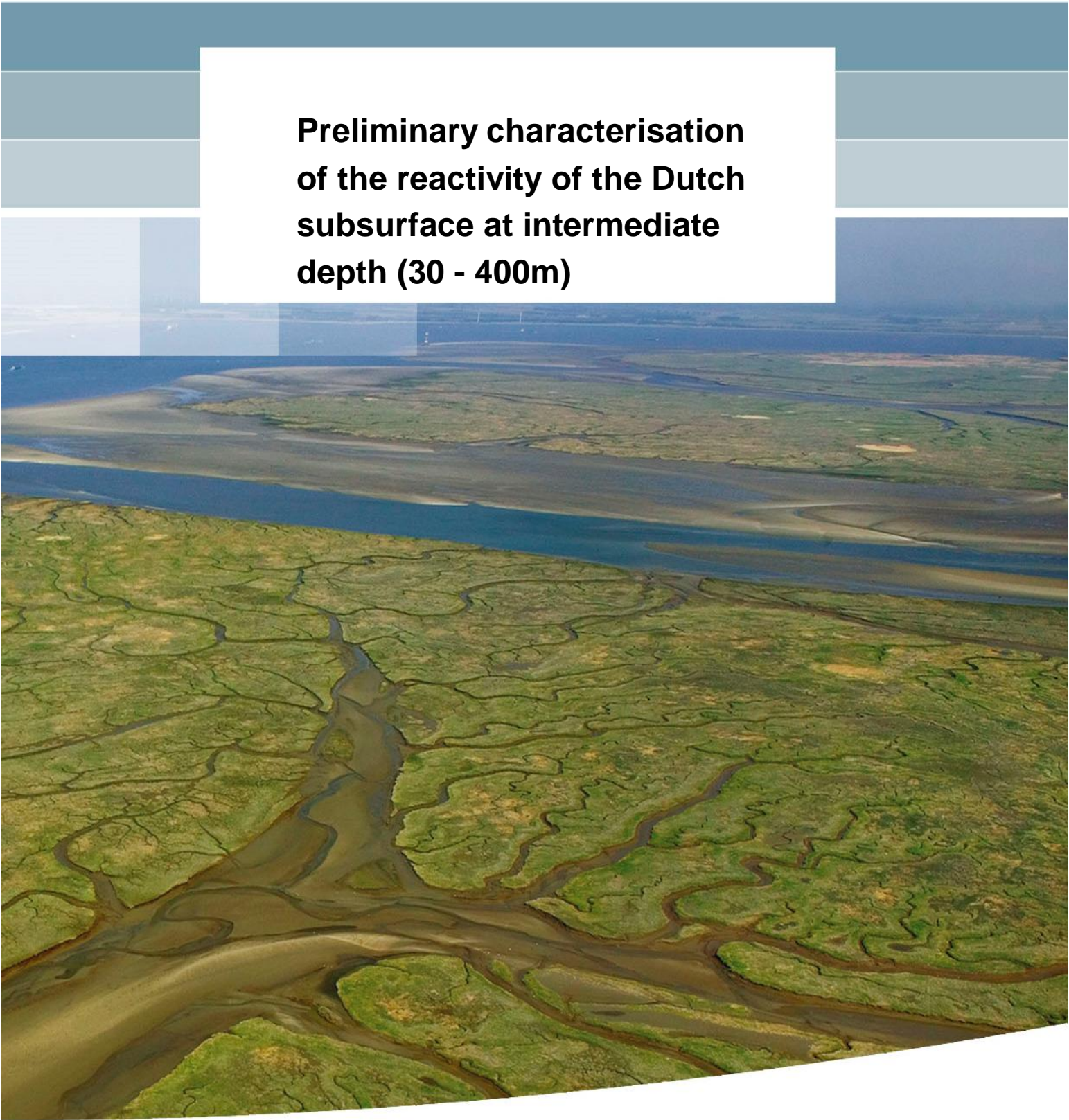


**Preliminary characterisation
of the reactivity of the Dutch
subsurface at intermediate
depth (30 - 400m)**



**Preliminary characterisation of the
reactivity of the Dutch subsurface at
intermediate depth (30 - 400m)**

Cheryl van Kempen
Jasper Griffioen

1207573-000

Title

Preliminary characterisation of the reactivity of the Dutch subsurface at intermediate depth (30 - 400m)

Project
1207573-000

Reference
1207573-000-BGS-0015

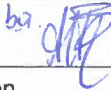
Pages
91

Keywords

Geological formation, characterisation, geochemical composition, sediment analysis, the Netherlands.

Summary

The objective of this study is to statistically characterise the geochemical composition of the Dutch subsurface at intermediate depth (30-400 m) as such characterisations were lacking before. Data-sets of geochemical analyses were obtained from TNO Geological Survey and drinking water company Vitens. Deltares integrated the data-sets into one database. 2700 samples were selected associated with 15 geological formations and classified on lithological class. The primary reaction capacity variables clay, Ca carbonate, pyrite, non-pyrite reactive Fe and elemental S were derived from the geochemical analyses together with the secondary variables cation-exchange capacity (CEC), total reduction capacity and carbonate buffering following acidification upon pyrite oxidation (CBPO). The characterisation obtained is preliminary because no rigorous quality control was performed. However, the results seem overall reliable and the statistical index numbers obtained are useful at the national scale. As anticipated, clay generally has higher averages in reaction capacities than sand. Marine sand is more reactive than riverine sand. Few data was available for formations other than marine or riverine ones. Correlation coefficients among the primary reaction capacity variables (as absolute values) are generally below 0.7, which implies that one variable cannot be estimated reliably from another variable. The obtained statistical index numbers can be used for groundwater transport simulations.

Version	Date	Author	Initials	Review	Initials	Approval	Initials
	jan. 2016	Cheryl van Kempen	by 	Johan Valstar		Hilde Passier	
		Jasper Griffioen					

State
final

Contents

1 Introduction	1
1.1 Background	1
1.2 Objectives	1
1.3 Realization	1
1.4 Explanation contentst	1
2 Collection of geochemical sediment analysis	3
2.1 TNO data collection	3
2.2 Data compilation	4
2.3 Geological formation classification	8
2.4 Geochemical calculations	9
2.4.1 Reaction capacity of sediments	9
2.4.2 Reactive and non-reactive iron	10
2.4.3 Pyrite	10
2.4.4 Clay fraction	11
2.4.5 Organic matter content	12
2.4.6 Lithology	12
2.4.7 Calcium-carbonate content	14
2.4.8 Secondary reaction capacity variables	14
2.5 Selection of data	15
2.6 Statistics	15
3 Results	17
3.1 Overview of the total dataset	17
3.2 Reaction capacity for intermediate depth	19
3.2.1 Data density	19
3.2.2 Marine formations	22
3.2.3 Riverine formations	24
3.2.4 Other formations	27
3.3 Secondary reaction capacity variables	30
4 Conclusions	33
5 References	35

Appendices

A Data sources	A-1
B Criteria per formation for different ranges in Al_2O_3 contents	B-1
C VBA code to edit detection-limits of elements	C-1
D SQL queries for calculating reactive capacities and selecting the data > 30m deep	D-1
E Geological cross-sections	E-1
F Statistics	F-1

1 Introduction

1.1 Background

For subsurface transport calculation for various applications, the knowledge about the geochemical composition of the subsurface is very relevant. We, therefore, need to know the average composition of the geological formations encountered and the related variability.

1.2 Objectives

The objective of this activity is to statistically characterise the geochemical composition of the geological formations in the Netherlands present at intermediate depth (30-400 m). This depth interval is chosen because systematic investigations are executed by TNO Geological Survey that deal with the GeoTOP, having its typical depth interval from the surface down to about 30 m depth. Reports about the statistical, geochemical characterisation of the geological units with the GeoTOP are present for regional areas that together largely coincide with the provinces of Groningen, Friesland, Drenthe, Zeeland, North- and South-Holland (Klein et al., 2012; Vermooten et al., 2011; Klein et al., 2015). Statistical, geochemical characterisations of the shallow subsurface of the Pleistocene Netherlands are presented by Bakker et al., 2007; Klein & Griffioen (2008), Groenendijk et al. (2008). Additionally, many geochemical projects have been executed during the last decades which results are available at TNO Geological Survey and Deltares.

1.3 Realization

Data-sets of geochemical analyses were obtained from TNO Geological Survey and drinking water company Vitens, that delivered geochemical analysis of samples collected around their winnings and analysed under responsibility of KWR to TNO Geological Survey. Many of the data of TNO were collected under the geological survey programs in the course of about 20 years. TNO and Vitens are thus owner of the geochemical data for almost all data-sets. Deltares integrated the data-sets into one database, that was further processed to obtain statistic data about the geochemical analyses.

1.4 Explanation contents

The set-up of this report is as follows. Chapter 2 presents the methods of data collection, handling and calculations in order to obtain a data set of geochemical analyses of the Dutch subsurface at intermediate depth. Chapter 3 presents the results and discussion and chapter 4 presents the conclusions. Appendix 1 through 4 present detailed aspects of the data handling, Appendix 5 presents two geological cross-sections at national scale for background information and Appendix 6 presents the statistical data of the various geological formations characterised.

2 Collection of geochemical sediment analysis

2.1 TNO data collection

The amount of data available for the deep subsurface of the Netherlands is relatively limited. A new dataset was compiled from data which came from different sources, but which was available at TNO through different projects which had been executed in the past.

The provenance of data can be summed up as coming from 8 different sources or projects. Table 1 lists these different data sources, the number of tables per source, the number of data-rows per source and the number of rows which were finally copied to the compiled database. Each data-row represents a unique xyz-location (location-depth combination). Because several datasets were in fact already compilations of data, the same data sometimes occurred in different datasets. These double occurrences were included only once, using the most complete dataset as a source or combining information of the two sources if it were complementary. This is the reason why the number of copied data-rows is smaller than the number of original rows.

Table 2.1. Data sources, original and copied rows and the sub-table names in which the data was collected.

	Data source	Tables	Original data-rows	Copied rows	Sub-table
1	Gunnink	1	6265	1785	Gunnink
2	Huisman	1	4962	4851	Huisman
3	TNO-data for STONE	17	1538	147	STONE
4	GC	2	283	247	Huisman
5	Sediment analyses Breda Formation	1	88	88	Huisman
6	Sediment analyses KWR Stuyfzand	7	191	188	KWR
7	ACME analyses	1	52	52	Huisman
8	Wubben	22	2984	2666	Wubben, Wubben_Parond
	Total		16363	10024	

Gunnink and Huisman are compiled datasets, containing data for many different locations. Gunnink however didn't contain measured values, but the 10-base logarithm of values. After recalculating the values, it turned out that many data-rows coincided with data from the Huisman dataset. The latter dataset was more complete, as it had SiO₂ analysis as well, which is why we preferred this dataset over the Gunnink dataset.

'**TNO-data for STONE**' coincided largely with data prepared by Wubben for inclusion in TNO's DINO portal. Both datasets include Parond 1 to 5 data.

'**Breda Formation**'-data comes from a single table, but different analysis methods were used to determine the same elements. To still be able to include all the data in the dataset, they were treated as if they came from different tables.

Almost every table had a different structure, and different column headings were often used. A large part of the time spent in this assessment was directed at modifying the tables so they had the same structure, column headings, units, etc. This could not be automated and was therefore largely done by hand. Some further optimization can still be made.

2.2 Data compilation

The process used to bring all the data together in a single '*basis*'-table will be described here. Between brackets are mentioned the column names in which the described information is stored. Also see table 2 and the following paragraphs for the 254 columns in our base-table.

Retrace ability

Each table was assigned its own unique code (FromTable) and for each data row the row-number in the table of origin was stored (mID). In principle for each cell in the table one should be able to look up the value in the original dataset with the FromTable and mID information. In some situations however, data occurred in several tables at the same time, while being complementary to each other. In these cases the most complete dataset was used where possible. In a few cases the information of the two sources was combined with the table name of the secondary table stored in the column (AlsIn).

Sub-tables

7 sub-tables were created, each collecting data from several sources which had largely the same structure and column names. The suitable (FromSubTable) in which data was collected can be *Gunnink*, *Huisman*, *Wubben*, *Wubben_Parond*, *STONE* or *KWR*. Finally the table names of these 7 sub-tables were edited so the tables could be merged to a single '*base*'-table.

Column names

Wherever possible original column names and the column the data was eventually stored in was recorded. In the case of data collected in subtables "Huisman, STONE and KWR", this was stored in excel-files in which the data was prepared for importing into access. In the case of "Wubben" and "Wubben_Parond", the original column headings are stored in the comments of the imported access tables.

The following column headings were finally included in our base-table. The number of columns we could include was limited by Access to 255 columns. Because information on detection limits was considered important to maintain in the same table, a number of other columns had to be left out. These columns often contain information for only a few data-rows and are therefore less important to maintain.

LocDepth_ID

This identification code is used to create an XYZ-location for each entry. It includes the BORING code and a depth at which the sample was taken. If this official TNO code wasn't available, then a LocDepth_ID was created based on other available codes, the source of the data or the XY locations. Where possible, the depth was included in the LocDepth_ID. If depth wasn't available, then the row number in the original data source was used. Depths used in the LocDepth ID generally represents the top of the column that was sampled. If this top-depth wasn't available, then the column's mid-depth was used, or if this too was unavailable, then the bottom-depth was used.

Table 2.2. How the LocDepth_ID – a unique code - was constructed and the number of rows with this type of code.

Type of code	From Table	rows
B{BORING}-{depth}		9401
X{X-coord}-Y{Y-coord}-{depth}	Amsterdam_AS	36
X{X-coord}-Y{Y-coord}-{depth}	Buizen_LUW	25
X{X-coord}-Y{Y-coord}-{depth}	Gr_BI_Slinger	14
{FromTable}-{depth}	Gemert	45
{FromTable}-{depth}	Huisman	58
{FromTable}-{mID}	CAL-GT-02_xrd_bulk	12
{FromTable}-{depth}	KWR_Roosteren	44
{FromTable}-{mID}	KWR_Someren	5
{Txx-xxx-x}-{depth}	Huisman	93
{Other Code}	KWR_WW_T4x	82
CAL-GT-02-XXX	CAL-GT-02	76
4300xxxx/x	Groeve Maalbeek	52

Table 2.3. The 254 Column-headings for our basis-table

column-heading	unit / remark
FromSubTable	Sub Table in which the data was collected prior to the final compilation
FromTable	Table of origin
AlsoIn	Table name of secondary source
mID	row-number in the table of origin
LocDepth_ID	Location-Depth code
BORING	TNO code
Bodemmeetpuntnummer {NITG}	Other TNO code
X coördinaat	X coordinate
Y coördinaat	Y coordinate
TNO-nummer	Other TNO code
ZKV	Sand, clay, peat
formatie (HvdM)	Formation (HvdM)
Auteur/analyst	Author, analyst
Project/gebied	Project / area
Opmerkingen	Remarks
monster/labcode	Labcode

Analyses	Type of analyses performed
Datum	Date
Labcode	2nd labcode
Top	m below surface
Bottom	m below surface
gem diepte	Average depth, m below surface
Diepte	depth used in LocDepth_ID
Maaiveld	surface elevation in m NAP
Formatie	Formation as determined in this assessment
Org C %	%
Pyriet	calculated pyrite from original table
Fe-reac	calculated reactive iron from original table
<p>For TGA the following columns were included: Residual weight, TGA for moisture (105) and 20-105, 105-450, 450-550, 550-800, 800-100 and 105-1000 trajectories.</p>	
<p>The following elements in % with information on detection limits: SiO₂, Al₂O₃, TiO₂, Fe₂O₃, MnO, CaO, MgO, Na₂O, K₂O, P₂O₅, S and Sum</p>	
<p>The following elements in ppm with information on detection limits: As, Cu, Pb, Zn, Ni, Cr, V, Sn, Sr, Ba, Rb, Ga, Zr, Nb, Y, Sc, La, Nd, Th, U, Li, Be, Na, Mg, Al, K, Ca, Ti, Mn, Fe, Co, Se, Mo, Ag, Au, Cd, Sb, Te, Cs, Ce, Pr, Sm, Eu, Gd, Tb, Dy, Ho, Er, Tm, Yb, Lu, Hf, Ta, W, Hg, Tl, Bi.</p>	
<p>Total C, TOC and S in %.</p>	
<p>Finally grain size information: Clay (< 2µm), <63µm, d(0.1), d(0.5), d(0.6), d(0.69) and the ratio d(0.6/d0.1)</p>	
<p>Grain size fractions with borders at (in µm): 0.01, 0.1, 0.2, 0.5, 1, 2, 4, 8, 16, 25, 35, 50, 63, 75, 88, 105, 125, 150, 177, 210, 250, 300, 354, 420, 500, 600, 707, 850, 1000, 1190, 1410, 1680, 2000</p>	
<p>Grain size fractions smaller than (in µm): 0.01, 0.1, 0.2, 0.5, 1, 2, 4, 8, 16, 25, 35, 50, 63, 75, 88, 105, 125, 150, 177, 210, 250, 300, 354, 420, 500, 600, 707, 850, 1000, 1190, 1410, 1680, 2000</p>	

Detection limits

In many cases tables only contained the mention 'below detection limit' without listing the detection limit for that assessment. This posed a problem, as often different detection limits are applicable for different analysis and detection limits can vary greatly between assessments. It is better to have an estimated value for these measurements than to set their concentration to zero or undefined. Therefore, detection limits (Table 2.3) were chosen based on the detection limits and data-averages of our own datasets, but also on detection limits found in other assessments (Klein et al., 2015).

Once a detection-limit was determined for all the data, 0.5 times that limit was added to the data-tables, to be used for reactive capacity calculations. Appendix 3 shows the VBA code which was used to calculate 0.5* the detection limit in Access.

Table 2.4. Choosing of detection-limit-values based on the entire dataset and other assessments.

nr	element	count of <dl ¹	chosen value ²	Table TNO ³	available Detection limits		available data	Avg ⁶
					DL_value ⁴	Frequency of DL_value ⁵		
1	SiO2	1	0.1	0.1				77.46
2	Al2O3	1	0.1	0.1				6.26
4	Fe2O3	70	0.004	0.008	0.004	2		3.13
5	MnO	37	0.001	0.001	0.01	43		0.20
6	CaO	38	0.0003	0.01	0.0003	1		3.02
7	MgO	113	0.002	0.002	0.002	20		0.55
9	K2O	1	0.006	0.006				1.43
10	P2O5	5	0.003	0.003	0.01	2		0.09
11	S	190	0.001	0.02 - 0.66	0.001	16		53.26
13	As	5	0.2	3	0.2	20		14.60
14	Cu	21	4	4	4	269		10.49
16	Zn	29	4	1	4	40		39.86
17	Ni	38	8	2	8	428		15.06
18	Cr	8	6	10	6	82		49.47
19	V	349	8	12	8	4		37.73
20	Sn	349	1	9	1	18		3.45
21	Sr	8	2	2				81.40
25	Zr	20	6	6				201.87
28	Sc	2	0.1	6	0.1	1		6.71
30	Nd	1	0.5	14	0.5	1		19.11
31	Th	106	0.5	9	0.5	10		6.54
32	U	99	0.2	3	0.2	21		1.48

Explanation of superscripts:

1. Number of times <dl occurs in our basis-table
2. Proposed value
3. DL in report by Klein et al. 2014 (Table 2-1)
4. Most frequent (or logical) value occurring in the basis-table
5. Frequency of that value
6. Average over all values

Other Mutations

The data of the tables had to be edited by hand and was checked several times to find duplicate data, errors, strange values or datasets using different units. These were corrected where possible. Many of these alterations were made by hand and were not recorded in detail. Hereunder follows a list of mutations which was generalized to give an impression of the kinds of alterations which had to be made:

- All data was checked to see if one LocDepth_ID had multiple occurrences. If so, the concentration data was checked for several elements to see if the data was duplicate. In that case, the data was removed. If the measured values were different, all rows were kept.
- Buizen_intterreg – monster/labcodes 1-6: BORING and LocDepth_ID were filled in based on the 'buisnummer'. The second letter in the middle of the code was left out so the code would coincide with the other BORING-codes.
- Negative values were treated as a detection limit or a value below detection limit.
- Surface altitude, top and bottom were converted to metres if they were in cm.
- LW_Texel (181 rows) did not have depth-information. This was added from STONE_Texel based on labcode.
- Whenever top-depth was missing, the average depth or bottom-depth was used for the LocDepth_ID.
- Whenever the BORING code was missing another code was used, the XY coordinates, or a code including the table name.
- For 3000 rows top and bottom were exchanged.
- For 3000 rows bottom and gem (average depth) were exchanged.

2.3 Geological formation classification

The TNO-codes and XYZ information were used to determine in which geologic formation each sample fits. For this the 3D model Digital Geological Model of TNO Geological Survey was used. The lithostratigraphic formations that are distinguished in the Netherlands are presented in the figure below together with their sedimentological settings. Reference is frequently made to these geological units in the remainder of this report. For 9400 data-rows, information about the geological formation could be added. For the remaining rows this was unfortunately not possible because the exact XYZ-location could no longer be determined.

Chrono-stratigrafie		Lithostratigrafische eenheden op formatieniveau							
		Marien	Fluviatiel				Glaciaal	Overig	
			Oostelijke rivieren	Rijn	Maas	Belgische rivieren			
Kwartair	Holocene	Formatie van Nasldwijk		Formatie van Echfeld	Formatie van Beegden	Krekrak Formatie		Formatie van Nieuwkoop	
		Eem Formatie		Formatie van Krefteneyne		Formatie van Koewacht	Formatie van Drente	Woudenberg	
	Pleistocene	"Midden"		Formatie van Urk				Formatie van Peelo	Formatie van Drachten
			Formatie van Appelscha	Formatie van Sterkzeel					
			Formatie van Peize	Formatie van Waaike					
	Pleistocene	"Vroeg"	Formatie van Maassluis						Formatie van Stramproy
	Neogeen	Pliocene	Formatie van Oosterhout			Kiezelooliet Formatie			
		Mioceen	Formatie van Breda			Formatie van Inden			
	Paleogeen	Oligoceen	Fm. v. Veldhoven						
		Rupel Formatie							
		Fm. v. Tongeren							
	Eocene	Formatie van Dongen							
	Paleoceen	Formatie van Londen							
							Formatie van Holsel		
							Formatie van Heljenrath		
							Formatie van Velle		

Figure 2.1. Scheme of the lithostratigraphic units that are distinguished in the Netherlands for the Cenozoicum.

2.4 Geochemical calculations

2.4.1 Reaction capacity of sediments

The reaction capacity of sediments encompasses a wide range of sediment properties, here we limit ourselves to a rigorous selection. Five so-called primary reaction capacity variables were identified as representing the most important components of the reaction capacity in sedimentary deposits (Van Gaans et al., 2011):

1. pyrite content;
2. total content of Fe in non-pyrite reactive compounds (oxides, siderite and glauconite);
3. clay fraction;
4. organic matter content and;
5. calcium carbonate content.

The primary reaction capacity variables were either analysed directly or calculated using chemometric equations (see below). Unfortunately, no distinction can be made a priori between ferrous and ferric Fe using the routine analysis applied. Whereas the sorption capacity for hydrophobic micro organics is dominantly controlled by organic matter content, several important reaction capacities are controlled by more than one (type of) solid compound. The following secondary reaction capacity variables were considered (for which chemo metric calculations are defined in the next section):

1. potential reduction capacity (PRC) by pyrite and organic matter,
2. cation-exchange capacity (CEC) by organic matter and clay content,

3. carbonate buffering upon acid production due to pyrite oxidation (CBPO) by carbonate and pyrite.

Surface complexation to humic and fulvic acids and to oxides can be assumed to be additive (e.g. Fest et al., 2005; Weng et al., 2001). The anion sorption capacity (ASC) is another secondary reaction capacity variable of interest. It is often overlooked, albeit of environmental relevance considering the fate of species such as phosphate, chromate and arsenic. It is also relevant within the framework of the fate of radionuclides as the most mobile and long-living radionuclides are oxyanions as iodide and Se as selenate or selenite. The ASC may be calculated from clay content and reactive Fe, where all reactive Fe is assumed to be Fe-oxyhydroxide and the role of aluminium oxides as anion sorbent is neglected. No reliable estimation of the anion sorption capacity from straightforward total element analyses is available, so any calculation must be considered as a rough estimate that is associated with a series of assumptions about the specific sorption capacity per unit weight of reactive solid.

2.4.2 Reactive and non-reactive iron

Total Fe and Al were analysed by XRF and for some series by ICP-MS following total destruction. Their contents are expressed on an oxide basis as % of total dry mass. Total Fe can be said to be present as Fe bound in non-reactive silicates (and some non-reactive oxides as chromite) and Fe bound in reactive minerals as siderite and Fe-oxyhydroxides. Non-reactive iron can be determined with empirically derived equations that assume a relationship with total Al as indicator for Al-silicates present:

$$\text{Fe}_2\text{O}_{3\text{non-reactive}} = \alpha * \text{Al}_2\text{O}_3 + \beta$$

where α and β are empirically determined coefficients for each (series of) formation (Heerdink & Griffioen, 2008), and Fe_2O_3 and Al_2O_3 are total Fe content and total Al content, respectively. The relation between non-reactive Fe_2O_3 and Al_2O_3 is different for Al_2O_3 contents > 5% compared to situation with contents < 5%. This is due to the dominance of feldspars and heavy minerals in the silt and sand fraction and that of clay minerals in the clay fraction. See Appendix 2 for the empirical values used. $\text{Fe}_{\text{non-reactive}}$ cannot be negative. The lowest value it can take is zero. Total reactive iron was then calculated using the following formula:

$$\text{Fe}_{\text{TR}} = 2 * \text{M}_{\text{Fe}} / \text{M}_{\text{Fe}_2\text{O}_3} * [\text{Fe}_2\text{O}_3 - (\alpha * \text{Al}_2\text{O}_3 + \beta)]$$

where Fe_{TR} is total reactive Fe. This formula assumes that silicate-bound Fe_2O_3 amounts to α times total Al_2O_3 content and that total reactive Fe could be viewed as an enrichment on top of the silicate-bound Fe (Dellwig et al., 2001; Dellwig et al., 2002; Huisman and Kiden, 1998).

2.4.3 Pyrite

Total S was analysed by X-ray fluorescence (XRF) and/or CS elemental analyser and expressed as % of total dry mass. Pyrite (FeS_2) content is calculated from the total S content. For non-peat samples,

$$\text{Pyrite} = 0.5 * \text{M}_{\text{FeS}_2} / \text{M}_{\text{S}} * \text{S}$$

While for peat samples TOC is used to correct for organic S, where a weight ratio between organic C and S is assumed of 110 to 1:

$$\text{Pyrite} = 0.5 * \text{M}_{\text{FeS}_2} / \text{M}_{\text{S}} * (\text{S} - \text{TOC}/110)$$

Next, Fe bound in pyrite is calculated as:

$$Fe_{py} = M_{Fe} * Pyrite / M_{FeS_2}$$

Fe bound in pyrite should be smaller or equal to total reactive Fe:

$$Fe_{py} \leq Fe_{TR}$$

and the non-pyrite bound reactive Fe (Fe_{reac}) can be calculated:

$$Fe_{reac} = Fe_{TR} - Fe_{py}$$

Otherwise, pyrite-bound Fe is corrected to equal total reactive Fe:

$$Fe_{py-corr} = Fe_{TR}$$

and non-pyrite bound reactive Fe is assumed to be equal to 0.

Finally, the amount of S in pyrite and the related pyrite content are calculated with

$$S_{py-corr} = Fe_{py-corr} * 2 * M_S / M_{Fe}$$

and

$$Pyrite = S_{py-corr} * M_{FeS_2} / (2 * M_S)$$

Relatedly, not all inorganic S (S_{in}) is bound in pyrite, which is assumed to be present as elemental S:

$$S^0 = S_{in} - S_{py-corr}$$

where S_{in} is 1. equal to total S for non-peat samples and 2. equal to total S corrected for organic S for peat samples (i.e., S- TOC/110).

The presence of gypsum or other Fe sulphides is neglected, which is justified for a combination of reasons. First, interpretation of incubation experiments based on reaction stoichiometry indicates that pyrite is dominantly present as reductant in different Dutch sediments (Hartog et al., 2002, 2005; Van Helvoort et al., 2007). Second, field studies on S speciation bring forward that iron sulphides other than pyrite are usually negligible in different kinds of sedimentary groundwater settings (e.g. Bates et al., 1998; Chambers and Pederson, 2006; Jakobsen and Cold, 2007; Massmann et al., 2004; Schwientek et al., 2008). Last, groundwater in the Netherlands is usually undersaturated for gypsum (Griffioen et al., 2013) and gypsum may only be observed in the unsaturated zone of reclaimed marine clays in polders following oxidation of pyrite and buffering by Ca-carbonate (Ritsema & Groenenberg, 1993).

2.4.4 Clay fraction

Grain-size fractions including clay fraction were determined by laser particle sizer and expressed as % of total dry mass. If grain-size information was available, then the following limits were used to determine the sand, silt and clay contents of a sample:

	Grain size range
Clay	<8 μ m
Silt	8 - 63 μ m
Sand	63 μ m to 2 mm

In the absence of grain size analyses, as is the case for most of the archive data, the clay fraction was calculated from the aluminum content. For all regions, an empirical equation was used based on the sediment analyses (for which $R^2 = 0.70$) in Griffioen *et al.* (2012) :

$$\text{Clay fraction (wt\%)} = 1.96 * \text{Al}_2\text{O}_3 \text{ (wt\%)} - 2.36 \quad (5)$$

where Al_2O_3 is total Al content of the sediment expressed on oxide basis and measured by XRF. If XRF- Al_2O_3 was not available, then Al based on total destruction and ICP-analysis was used. The intercept in this formula is explained by the presence of feldspar minerals as major Al-bearing constituent in sandy sediments having low Al_2O_3 in addition to Al-bearing clay minerals that become more prominent with increasing clay content.

2.4.5 Organic matter content

Organic Matter content was determined in one of three ways:

Total Organic Carbon (TOC) was measured by means of a CS elemental analyser, after removal of carbonates. Additionally or alternatively, organic matter (OM) was analysed using thermo-gravimetric analysis (TGA). Both are expressed as a % of total dry mass. When necessary, organic carbon was converted into organic matter taking a factor of 2 into account. Organic matter was determined as follows:

1. If available, TOC from CS elemental analyser was used, taking a factor of 2 into account: $\text{OM} = 2 * \text{TOC}$
2. Else results from thermo-gravimetric analysis (TGA) were used, and the following formula: $([\text{TGA } 105\text{-}450] + [\text{TGA } 450\text{-}550]) - 0.07 * \text{Clay}$.

2.4.6 Lithology

The lithological class was determined according to a sequence of rules. In first instance, the grain-size analysis was used to determine the lithological class. Second, the clay content was calculated from the Al_2O_3 content and used for classification. Third, the lithological description available was used and finally, remaining samples were always classified as sand. Clay, Loam, Sand and Peat lithologies (Klei, Leem, Zand and Veen respectively in Dutch) can be determined using the Clay-Loam-Sand triangle and the Peat triangle. All samples for which no lithology was known after these assessments, were treated as sand-samples.

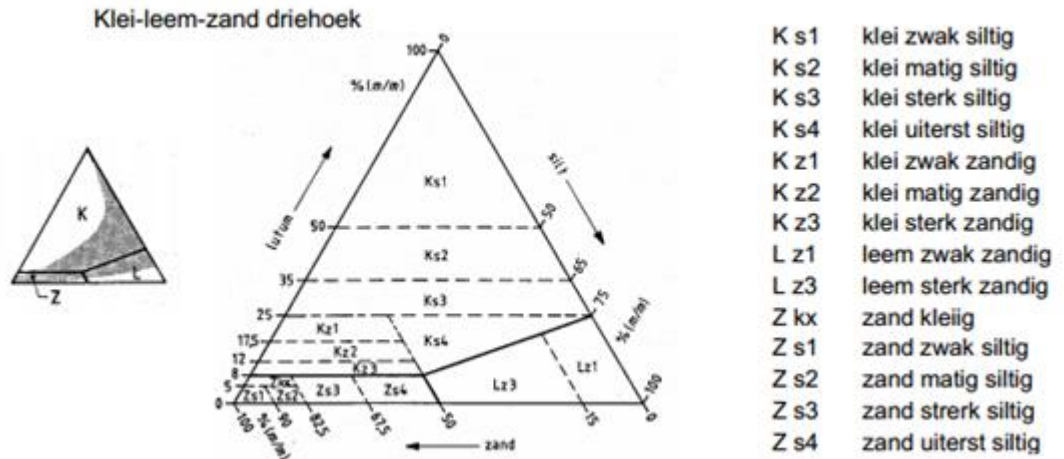
Sand/Loam/Clay are determined based on the clay, silt and sand-fractions, normalized in such a way that together they sum up to 100%. The normalized SLC-values and the triangle can then be plotted in an XY-plane with the following formulae:

$$Y_{\text{slc}} = \text{Clay}_{\text{slc}} * \sin(\alpha)$$

$$X_{\text{slc}} = Y / \tan(\alpha) + \text{sand}_{\text{slc}}$$

where $\alpha = 1/3 * \pi$

The X-axis coincides with the sand-axis as shown in the triangle in figure x, while the Y-axis is perpendicular to it. If sand > 50% and Clay < 8%, the sample is sand. If sand < 50%, but Y_{SLC} falls below the Loam-Clay-boundary, then the sample is loam. In the other cases, the sample consists of clay.



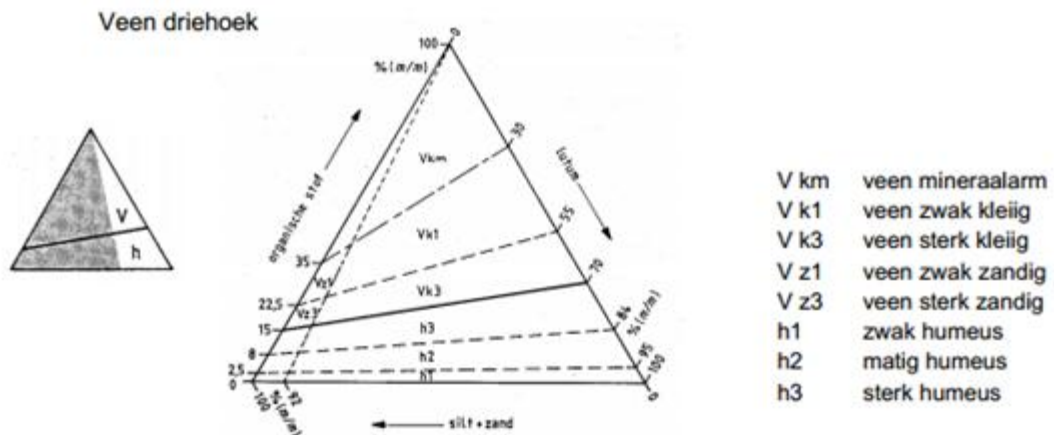
Whether a sample comes from a peat-environment is similarly determined, but this time organic matter (OM), clay and silt+sand together add up to 100%.

$$Y_{\text{peat}} = OM_{\text{peat}} \cdot \sin(\alpha)$$

$$X_{\text{peat}} = Y_{\text{peat}} / \tan(\alpha) + (\text{silt}_{\text{peat}} + \text{sand}_{\text{peat}})$$

Where $\alpha = 1/3 \cdot \pi$

If Y_{peat} is higher than the humic-peat-boundary, then the sample consists of peat.



Second, samples for which only the clay content was available were arbitrarily assigned a lithology:

- < 8% clay was assigned sand
- >8% clay was assigned clay

The clay percentage may be calculated from the Al_2O_3 content (see section 2.3.1.3).

Third, whenever Clay, Loam, Sand and Peat had been reported in the tables, this was copied to our basis-table. If all this information was not available, the sample was classified as sand.

2.4.7 Calcium-carbonate content

Carbonate was derived from TGA measurements with the following formula:

$$\text{Carb} = \frac{\text{TGA}_{800} * M_{\text{CaCO}_3} / M_{\text{CO}_2}}{\text{TGA}_{800} * 100 / 44}$$

Alternatively, carbonate can be calculated from total Ca analysed as % CaO by XRF. In the latter case, comparably to Fe, the silicate-bound Ca is subtracted from the total Ca using an empirical formula:

$$\text{Carb} = M_{\text{CaCO}_3} / M_{\text{CaO}} * [\text{CaO} - (0.0448 * \text{Al}_2\text{O}_3 - 0.1147\%)]$$

where Carb is carbonate and CaO is total Ca content. The calculation only considers Ca-carbonate whereas in TGA dolomite, Mg-bearing calcite and ankerite are included as well (Milodowski et al., 1989; Warne et al., 1981). The two procedures are thus not strictly equivalent.

2.4.8 Secondary reaction capacity variables

The *secondary reaction capacity variables* were calculated from the primary reaction capacity variables using stoichiometric or pseudo-stoichiometric relationships. Probably more compounds can influence the reaction capacities mentioned, but only the most important ones are indicated.

The *potential reduction capacity* (PRC in el/kg) takes into account organic matter and pyrite as major reductants (Barcelona and Holm, 1991; Hartog et al., 2002):

$$\text{PRC} = 10 * [15 \text{FeS}_2 / M_{\text{FeS}_2} + 2 * \text{OM} / M_{\text{C}}]$$

where the factor 10 is a dimensionless constant for the conversion from % to el/kg dry mass. The cation exchange capacity (CEC in meq/kg) is calculated using an empirical relationship derived for fluvial sediments (Van Helvoort, 2003), where distinction is made between organic-rich and organic-poor sediments (with 20% organic matter as criterion):

$$\text{CEC} = 4.0 * \text{clay fraction} + 12.5 * \text{OM} \quad \text{OM} < 20 \% \text{ dry weight}$$

$$\text{CEC} = 2.7 * \text{clay fraction} + 15.2 * \text{OM} \quad \text{OM} > 20 \% \text{ dry weight}$$

The pseudo-stoichiometric multipliers also account for a conversion from % to mg/kg dry mass. Carbonate buffering upon pyrite oxidation (CBPO in mmol/kg) takes into account the acid buffering capacity of carbonate following pyrite oxidation by O₂:

$$\text{CBPO} = 10,000 * \left[\text{CaCO}_3 / M_{\text{CaCO}_3} - 2 * \text{FeS}_2 / M_{\text{FeS}_2} \right]$$

Again, the factor 10,000 is a dimensionless constant for the conversion from % to mmol/kg dry mass. It should be noted that in the newly collected dataset of the Pleistocene area, all samples were analysed by XRF, CS elemental analyser, laser particle sizer, and TGA. In contrast to the archive datasets, therefore, this new dataset is consistent and all primary and secondary variables were calculated in the same way.

2.5 Selection of data

For the current analysis a subset was extracted from the basis-table, containing only data of 25m and deeper. Data which fell in the 25 to 30m interval was later removed, except for data from a few boreholes which also had measurements at 30m or deeper if this would add to the quality of the statistics we would derive.

Data was also removed if there were too few measurements for calculating meaningful statistics. Statistics were only calculated for formations for which more than 9 samples were available. Because the number of Peat and Loam samples was very limited, no statistics could be determined for these lithologies. Statistics were determined for Clay and Sand.

2.6 Statistics

Statistics per formation were determined using the PRCtool, developed by Heerdink (2009). The PRCtool gives general statistics for a dataset, giving insight into the frequency distribution, average and standard deviation of the data. In our case these statistics were determined for each formation and for the whole of the Netherlands. The results are 50, 17.5 and 82.5 percentiles, the average and standard deviation of the data. These results are presented in a table, and plotted in graphs for Clay and Sand. Graphs are only plotted if more than 20 samples are available.

3 Results

The statistical results are presented in this chapter. Two geological cross-sections across the Netherlands are presented in Appendix 5 in order to obtain an idea about the position of the geological formations. Two general remarks must be made: first, the Digital Geological Model majorly addresses the geological units of the Miocene Breda Formation and younger. Older Paleogene units are only addressed in DGM when they are close to the surface. Second, one may note the considerable thickness of the Neogene and Early Pleistocene formations compared to those on top of them. The Neogene and Early Pleistocene formations may thus play an important role in the safety function of subsurface disposal of radioactive waste.

3.1 Overview of the total dataset

The full dataset compiled in this assessment contains 10024 data-rows for 9742 unique depth-location-combinations, or 1171 unique XY locations. For the following elements, more than 5000 data-rows are available:

SiO₂, TiO₂, Al₂O₃, Fe₂O₃, MnO, CaO, MgO, Na₂O, K₂O, P₂O₅, Ni, Ba, V, Sr, Zr, Cr, Y, Zn, Cu, S, Pb, As, Rb, Ga, Nb, U, Th.

For all other elements around 1000 data-rows are available, except for the rare earth elements, for which only 100 data-rows are available.

Data herkomst en maximum-diepte van de boring.

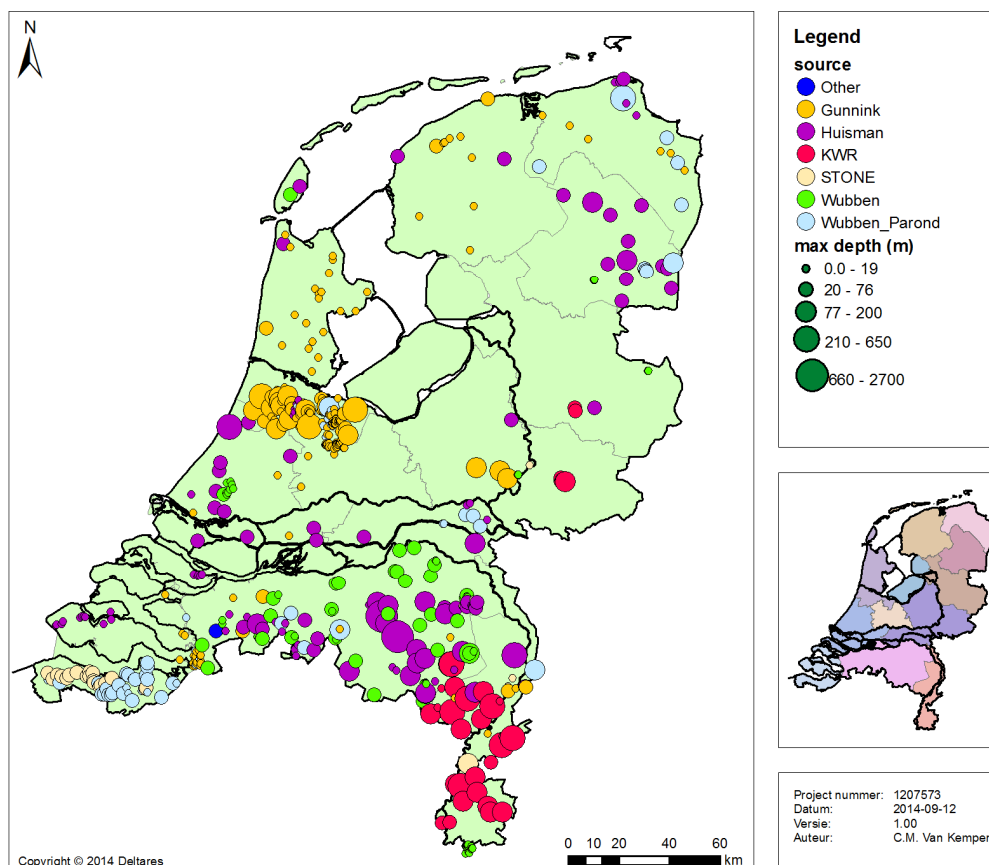


Figure 3.1. Location and depths of the drillings from which samples were collected, geochemically analysed and processed in this study.

Samples were classified by lithology using grain size analysis, the visual observation or Al_2O_3 content as proxy for clay content. The results are presented in Figure 3.2 for those samples for which grain size analysis was executed. It is clear that few peat samples are present and most samples are clastic with up to several percent organic matter. Classification of sediments on lithology suggests discrete classes but the data clearly show a continuum from sand-rich to silt- and clay-rich. The ensemble of samples is majorly restricted to a narrow spectrum. This narrow spectrum has been observed in other data-sets of Dutch soils and sediments as well (Bosch et al., 2014).

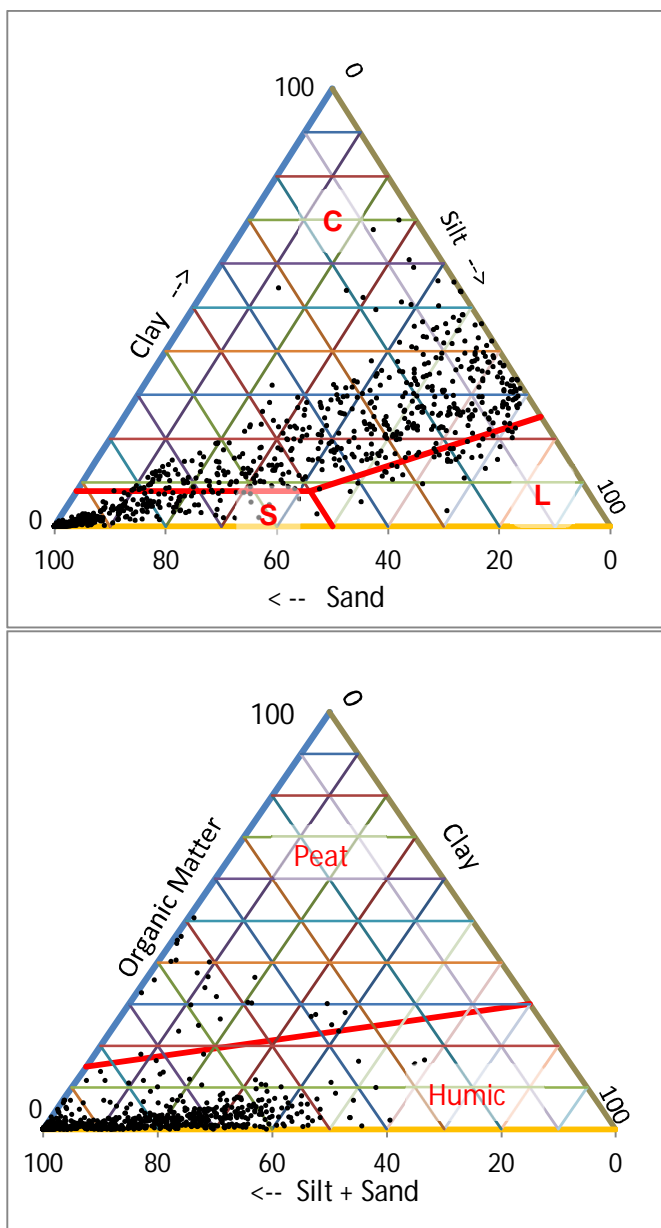


Figure 3.2. Samples plotted in the Sand-Clay-Loam triangle (above) and the Peat triangle (below).

3.2 Reaction capacity for intermediate depth

3.2.1 Data density

Samples from a depth of 30 m and more were selected for further statistical analysis. Reference is made to a series of reports and the related publications for statistical characterisation of the first 30 m depth, i.e., the GeoTOP (Bakker et al., 2007; Klein & Griffioen, 2008; Groenendijk et al., 2008; Van Gaans et al., 2011; Vermooten et al., 2011; Griffioen et al., 2012; Klein et al., 2012; 2014). In order to keep samples from a trajectory in a drilling together, we also investigated whether a geological formation present below 30 m depth had its upper boundary between 25 and 30 m depth. If this holds, we added the samples collected from this trajectory to the other samples selected. In this way, the data-set per geological formation becomes somewhat bigger and a better insight becomes obtained in the vertical heterogeneity of the formations. Table 3.1 presents the drillings and geological formations for which this holds. We avoided to select shallower samples because these have been more likely subject to leaching by infiltration of rain water: substantial changes in groundwater pH or redox state are usually observed within the first 25-30 m of the Dutch subsurface (Broers, 2002; Fest et al., 2007; Griffioen et al., 2013). The number of peat samples was only 7 and they were not considered any further. Several geological formations had less than 9 samples selected (Table 3.2), which were also excluded for further statistical analysis.

Table 3.1. Boreholes with relevant data in both the 25-30 m trajectory and > 30 m, selected to improve our dataset.

Formation	Borehole	count
KR	B30G08	11
KR	B31D01	14
KR	B34C01	3
PE	B03G01	3
PE	B11F01	2
PE	B12D00	4
PE	B17G00	4
RU	B53F00	1
RU	B54A00	2
RU	B54B00	1
RU	B54E03	2

Table 3.2. Formations not assessed because they had less than 9 samples.

Abbreviation	Formation	Count
BE	Beegden	6
DO	Dongen	6
DR	Drenthe	7
EE	Eem	8
GU	Gulpen	2
HT	Heijenrath	3
MT	Maastricht	2
TO	Tongeren	4

Table 3.3 presents the numbers of samples selected grouped in terms of geological formation and lithological class. 2700 samples were selected in total and distributed across 16 geological units. Comparison with Figure 2.1 indicates that all major Oligocene, Early and Middle Pleistocene formations are represented except the Beegden Formation. This formation, however, lies often within 30 m depth and down to 50 m at most in the southeastern part of the Netherlands (www.dinoloket.nl). The sub-set selected thus covers the Dutch subsurface at intermediate depth, where it is a priori unknown how representative this sub-set is. The amount of samples per geological unit varies from 66 for the Rupel Formation to over 800 for the Peize/Waalre Formations. The Boom Clay has been extensively characterised by Koenen & Griffioen (2014) based on about 150 samples mostly from northern and southern Netherlands. This characterisation may be preferred over the present one for the Rupel Formation, where it should be noted that the two characterisations are based on entirely different sample sets.

Table 3.3. Formations with more than 9 samples and therefore eligible for calculating statistics (M. means member)

Formation	Name	Type	Lithology			Total
			C	L	S	
AP	Appelscha	Riverine	1		53	54
BR	Breda	Marine	82	5	30	117
BX	Boxtel	Other Formations	22		32	54
DT	Gestuwd	Other Formations	46		42	88
KI	Kiezelooyet	Riverine	34		35	69
KR	Kreftenheye	Riverine	8		45	53
MS	Maassluis	Marine	115		132	247
N	Base of the North Sea Group	Marine	46		16	62
OO	Oosterhout	Marine	160	3	161	324
PE	Peelo	Other Formations	15		38	53
PZWA	Peize Waalre	Riverine	381	5	483	869
RU	Rupel	Marine	26		7	33
ST	Sterksel	Riverine	76		191	267
SY	Stramproy	Riverine	118		70	188
URTY	Urk, Tijnje M.	Riverine	103		16	119
URVE	Urk, Veenhuizen M.	Riverine	30		73	103

The figures for the lithological classes indicate that, as expected, most samples are clay or sand. The amount of loam samples is overall low: only 13 samples from 3 formations. This data was not processed using the PRCTool and considered any further. Figure 3.3 presents a map with the locations of the drillings from which samples were selected. Three areas show high densities: 1. Zeeuws Vlaanderen in the southwestern Netherlands, 2. the Roer Valley Graben and part of Limburg south of it and 3. southern part of Noord-Holland province with immediate vicinity. The maximum depth of the series of samples is almost 400 m and the average depth is 91 ± 79 m. Most samples lie thus within 150-200 m depth. The statistical results are presented in Appendix 6 as cumulative frequency diagrams and related tables with three representative percentile values, averages and standard deviations. The amounts of data for clay and Ca-carbonate contents are much higher than for pyrite, reactive Fe and

organic matter because XRF-analysis was most frequently done (but total-S was not reported because this element is not determined very accurately by XRF). Unfortunately, few or no CS-elemental analysis and TGA analysis were performed or other analytical techniques that yield data for organic matter, pyrite and reactive Fe other than pyrite. Statistical characteristics of one formation may thus have been assumed representative for other formations that have a comparable sedimentological origin and geological history.

Data origin and max-depth of the borehole

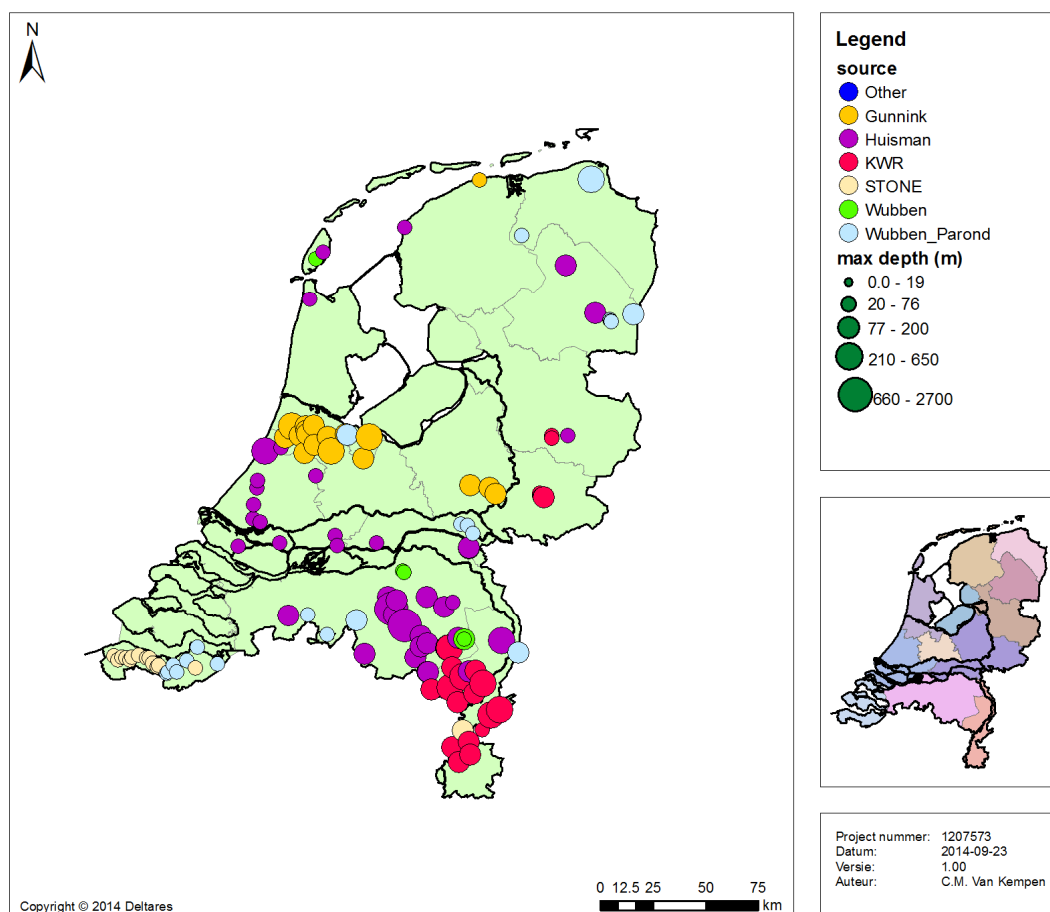


Figure 3.3. Data origin and max-depth of the boreholes for data >30m: 129 drilling locations

Note that the 17.5 and 82.5 percentile values lie 65 % away from each other, which is equal to two times the standard deviation for a normal distribution. These two percentile values provide a good indication of the spreading around the median for non-normally distributed data-sets. Usually, the average is larger than the median, the standard deviation is repeatedly larger than the average and the median lies close to the 17.5 percentile value (which may be close to or below the detection limit). This emphasises the non-normal character of the data-sets. It also stresses that average values may be a better, first characterisation of the overall reactivity of a formation than median values: a limited fraction of the sediment with high contents determines the average reactivity in the deep groundwater compartment where groundwater residence times are rather long. This holds in particular for sand where the majority of the samples may have contents close to or below the detection limit and thus limited or no reactivity.

From a geohydrological point of view, the question is open how the statistics for sand and clay should be combined to an overall characterisation of the reactive properties of a

geological formation. Groundwater will preferably follow the most permeable strata, which will be sandy. Flow through clayey strata will be mostly vertical and flow through sandy strata can be more horizontal and at length. The data will be described in three parts according to the origin of the sediment: marine, fluvial and other.

3.2.2 Marine formations

The averages and standard deviations of the primary reaction capacity variables are presented in Table 3.4 for sand and clay in the marine formations. As one would expect, the reactivity of clay is larger than of sand. A notable exception is the reactive Fe content for the Breda and Oosterhout Formations: this is higher in sand than in clay, which suggests that the redox state in these clays has been more often SO₄ reducing than in these sands.

Table 3.4. Average contents with related standard deviations (in wt%) of the primary geochemical variables in the marine geological formations as present at intermediate depth.

Formation	clay	Ca-carbonate	org. matter	pyrite	reactive Fe	elemental S
sand						
RU						
N	5.5 ± 1.9	11.2±8.0	0.8 ± 0.4			
BR	3.7 ± 2.3	0.4±0.7	0.3 ± 0.7	0.1 ± 0.2	4.1 ± 4.7	0 ± 0
MS	2.5 ± 1.9	5.5±4.8				
OO	3.2 ± 2.3	5.8±12.4	0.3 ± 0.3	0.4 ± 0.5	0.7 ± 1.1	0 ± 0.1
clay						
RU	16.2 ± 8.4	24.3±65.1	1.3 ± 1.1			
N	10.9 ± 1.6	6.6 ± 2.4	1.3 ± 0.2			
BR	22.8 ± 7.1	6.7 ± 11.7	2.0 ± 0.8	0.5 ± 0.5	0 ± 0.1	0.5 ± 0.3
MS	19.4 ± 4.9	13.2 ± 8.7				
OO	22.8 ± 7.8	9.9 ± 7.3	0.7 ± 0.3	1.2 ± 1.6	0.2 ± 0.6	0.3 ± 0.4

Table 3.5. Correlation coefficient between clay content and other primary reaction capacity variables for the marine formations.

ALL (n = 747)	Ca carbonate	org. matter	pyrite	reactive Fe	elemental S
RU	0.085	0.534			
N	-0.522	0.613			
BR	0.254	0.459	0.044	-0.428	0.426
MS	0.394				
OO	0.035	0.545	0.152	-0.279	0.668
Only clay (n = 408)					
RU	-0.027	0.384			
N	-0.007	0.533			
BR	-0.174	0.062	-0.281	-0.317	0.070
MS	-0.254				
OO	-0.507	0.428	-0.573	-0.347	0.646

The correlation between clay and the other primary reaction capacity parameters has been calculated per geological formation for both the total data set and only the clay samples. With 408 out of 747 samples, the fraction of clay samples is somewhat above 50%. The results are presented in Table 3.5. The coefficients are mostly low and frequently negative. Negative correlation coefficients may be expected between clay and Ca carbonate contents in sediment when Ca carbonate is high and goes on the expense of clay. This seems to hold for the clay sediments of the Maassluis and Oosterhout Formations (Figure 3.4). Some of the high coefficient are due to very small numbers of samples as for, in particular, elemental S. Visual inspection in scatter plots confirms these observations and also points out that most data are not strongly grouped around a centre (Figure 3.4). Noteworthy is the gap in organic matter content for the Breda samples: contents are either below 1% or above 1.8%. One implication is that for the latter, organic matter contributes to the CEC in addition to clay (cf. the equation for CEC in section 2.3.1.7).

The implication of small correlation coefficients is that 1. the other primary reaction capacity variables cannot be well estimated from clay content and 2. the secondary reaction capacity variables are strongly uncorrelated with the individual primary variables when the two primary variables involved contribute both substantially to the secondary variable. Correlation coefficients were also calculated between organic matter and pyrite contents because other Dutch studies (Heerdink & Griffioen, 2012; Klein et al., 2015; Griffioen et al., 2016) indicate that pyrite frequently occurs in association with sedimentary organic matter because this is the substrate for SO_4 reduction. The coefficients were smaller than 0.4 and thus low, irrespective whether the formation as a whole was considered or only clay.

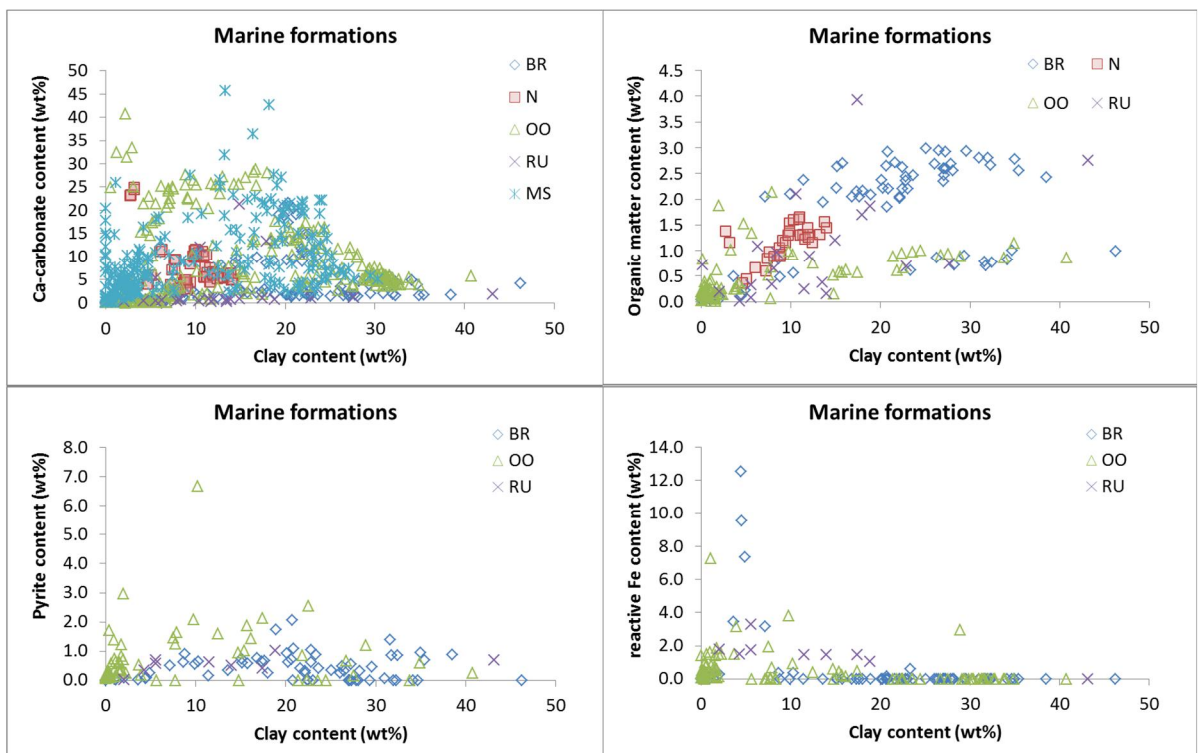


Figure 3.4. Scatter plots between clay content and the other primary reaction capacity variables for the marine formations. Three sand samples with extreme Ca-carbonate contents between 50-70 % are not plotted in the upper, left graph.

Figure 3.4 confirms that the highest reactive Fe contents are found in sand and not clay, where extreme contents up to 12% are found in the Breda Formation. This is likely glauconite-rich sand, which is commonly found in the Breda Formation. Glauconite is an Fe rich clay mineral that is authigenically formed in marine sediments. Figure 3.5 characterises the relationships between reactive Fe, pyrite and elemental S. The highest reactive Fe contents are found when pyrite is low and conversely. For many samples, elemental S and pyrite exclude each other while the contents are clearly above the detection limit of about 0.1 %. Total reactive Fe is thus frequently too low in the sediment in order to produce pyrite during SO₄ reduction. Instead, elemental S became produced under these conditions. Comparison with clay content, points out that this situation is rather restricted to clay sediments.

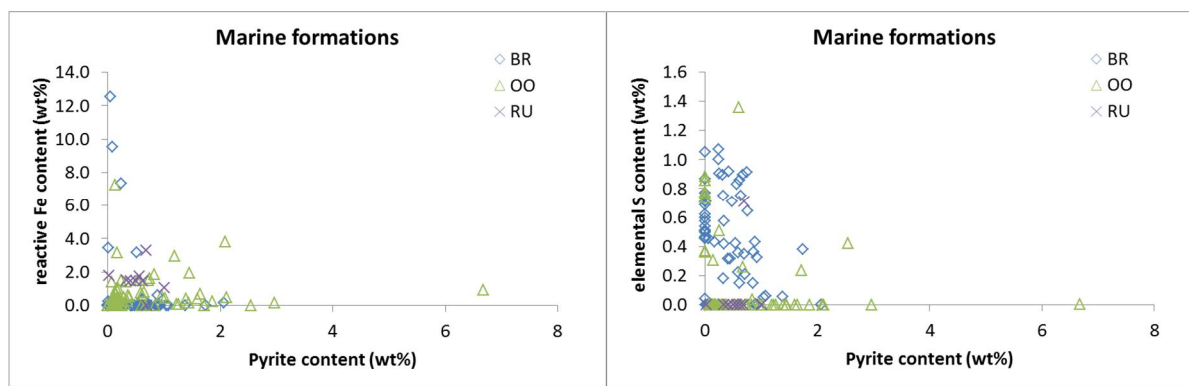


Figure 3.5. Scatter plots between pyrite and the related reactivity variables reactive Fe and elemental S for the marine formations.

3.2.3 Riverine formations

The averages and standard deviations of the primary reaction capacity variables are presented in Table 3.6 for sand and clay in the riverine formations. The reactivity of clay is larger than of sand, like for the marine formations. However, reactive Fe content is not an exception for the riverine formations. Overall, the values of the averages are lower for the riverine formations than for the marine formations, except for clay, organic matter and reactive Fe contents in clay. Riverine sand is thus less reactive than marine sand.

Table 3.6. Average contents with related standard deviations (in wt%) of the primary geochemical variables in the riverine geological formations as present at intermediate depth.

Formation	clay	Ca carbonate	org. matter	pyrite	reactive Fe	elemental S
	sand					
AP	0.3 ± 0.5	0.1 ± 0.2	0.1 ± 0.2	0 ± 0.1	0 ± 0.1	0 ± 0
KI	1.3 ± 1.8	7.1 ± 27 [#]				
KR	1.7 ± 1.4	2.0 ± 2.0				
URVE	4.0 ± 2.5	3.5 ± 3.8				
URTY	2.9 ± 2.5	7.9 ± 8.8	0.5 ± 0.6			
SY	1.2 ± 1.8	2.1 ± 5.5				
ST	3.4 ± 2.2	2.3 ± 2.8	0.5 ± 2.3	0.2 ± 0.3	0.3 ± 0.4	0 ± 0
PZWA	2.3 ± 2.3	1.3 ± 2.7	0.1 ± 0.2	0.1 ± 0.1	0 ± 0.1	0 ± 0.1
	clay					
AP						
KI	27.7 ± 11.3	40.6 ± 60.1 [#]			0 ± 0	
KR	16.7 ± 12.8	2.1 ± 3.6				
URVE	15.4 ± 6.6	10.1 ± 5.0	0.7 ± 0.8			
URTY	17.4 ± 5.8	17.3 ± 17.3	3.0 ± 2.8			
SY	17.3 ± 5.7	3.5 ± 6.2	3.3 ± 4.8	0.8 ± 1.2	0.6 ± 0.8	0.1 ± 0.4
ST	16.2 ± 5.7	11 ± 7.7	1.0 ± 0.6	0.3 ± 0.2	2.0 ± 1.2	0 ± 0
PZWA	19.0 ± 5.6	7.0 ± 8.2	2.2 ± 4.6	0.3 ± 0.4	0.2 ± 0.7	0.2 ± 0.6

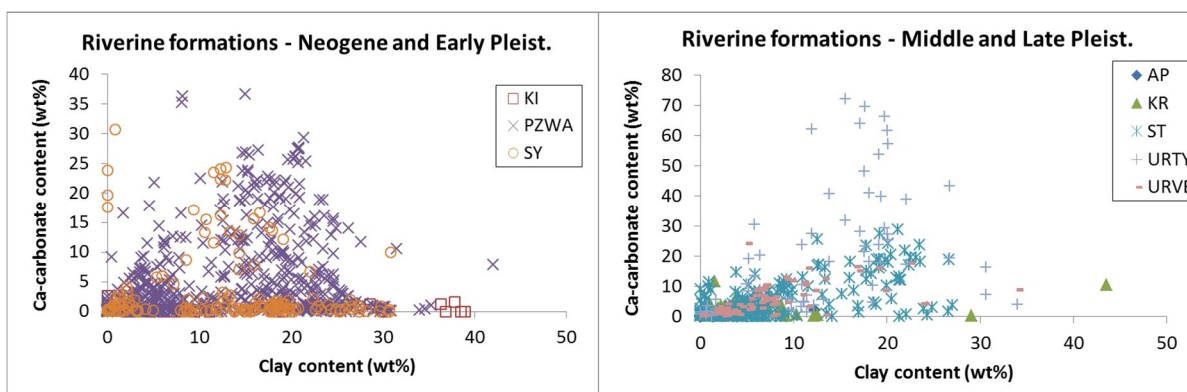
unreliable statistics due to erroneous values for Ca-carbonate content in several samples

Table 3.7 presents the correlation coefficients between the clay content and the other primary reaction capacity variables. The erroneous Ca-carbonates in some of the Kiezeloolliet Formation samples were excluded in the related calculations. The majority of the riverine samples are sandy and, therefore, the correlation coefficients associated are also calculated. The values vary strongly and absolute values above 0.7 happen regularly. The highest values for pyrite and reactive Fe in the Appelscha Formation are strongly determined by many 0 values for all three variables involved and give a misleading impression. The correlation coefficient between organic matter and pyrite contents is 0.638-0.940 for the Appelscha, Sterksel and Stramproy Formations and 0.103 for the Peize/Waalre Formation. The latter changes to 0.608 when only the sand samples are considered. These observations indicate that an association may exist between pyrite and sedimentary organic matter as its likely substrate in these riverine formations.

Table 3.7. Correlation coefficient between clay content and other primary reaction capacity variables for the riverine formations (groups with less than 10 samples were not considered).

ALL (n = 1610)	Ca carbonate	org. matter	pyrite	reactive Fe	elemental S
AP	0.772	0.736	0.981	0.983	-0.227
KI	0.219	0.568			0.622
KR	0.349	0.305			-0.644
PZWA	0.364	0.396	0.339	0.098	0.330
ST	0.658	0.116	0.158	0.873	-0.110
SY	-0.011	-0.020	-0.037	0.227	-0.303
URTY	0.428	0.548			
URVE	0.576				
ONLY SAND (n = 966)					
AP	0.234	0.723	0.715	0.651	-0.348
KI	-0.177				
KR	0.416	0.305			-0.644
PZWA	0.419	0.323	0.423	0.316	0.293
ST	0.254	0.052	0.300	0.384	-0.108
SY	0.010				
URTY	0.818	0.311			
URVE	0.589				

The scatter plots indicate that the Ca-carbonate contents strongly scatter for clay: amounts up to 30% are not uncommon and higher values are even found in the Tynje member of the Urk Formation (Figure 3.6). Inspection of the data brings forward that these high CaO contents go together with high MgO and P₂O₅ contents, which are associated with carbonates, and the sum of metals expressed as oxide is below 100%. This implies that there is no reason to disbelieve these extremely high Ca-carbonate contents. The scatter plots emphasise that there is a notable difference in organic matter content between sand and clay (criterium 8% clay): contents above 1% are rare for sand but not for clay. The plots further indicate that pyrite contents are usually below 1% (and also elemental S; Figure 3.7), whereas reactive Fe is frequently 0% but contents up to a few percent also happen particularly in clay. Elemental S and pyrite exclude each other for many sediment samples and reactive Fe and pyrite do less.



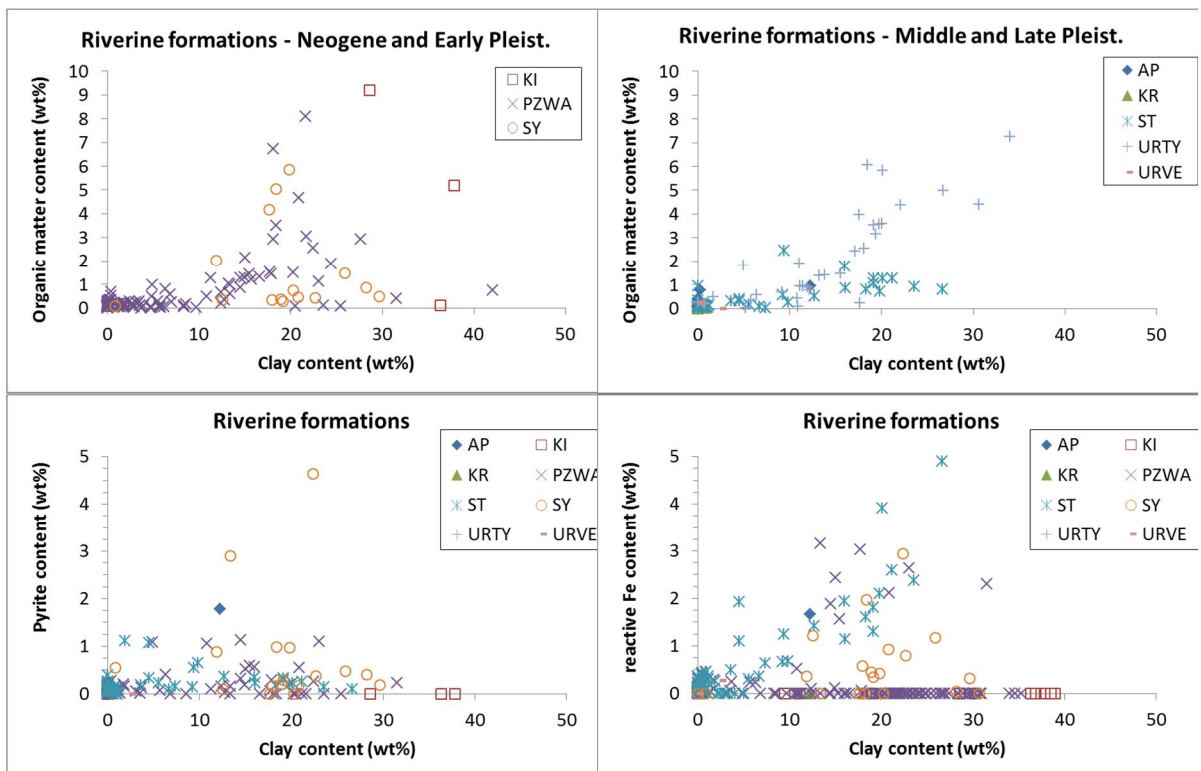


Figure 3.6. Scatter plots between clay content and the other primary reaction capacity variables for the riverine formations.

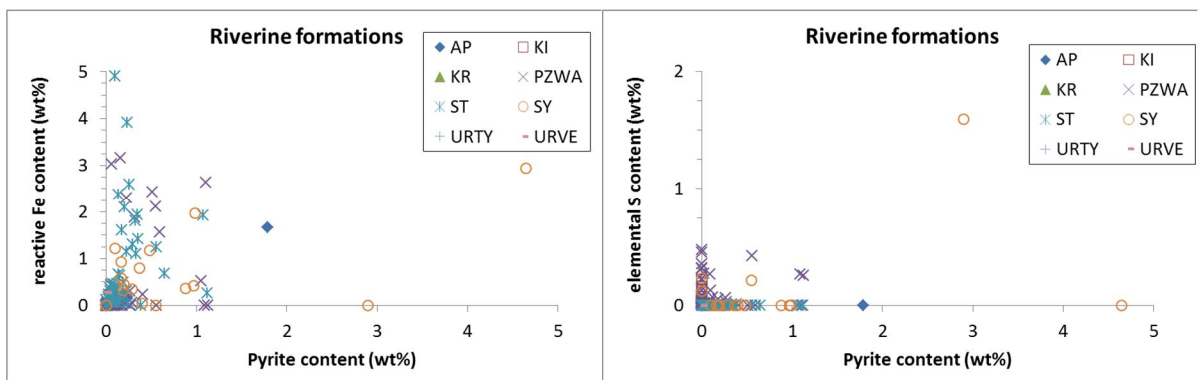


Figure 3.7. Scatter plots between pyrite and the related reactivity variables reactive Fe and elemental S for the riverine formations.

3.2.4 Other formations

With about 160 samples, this data group is much smaller than the data groups for the marine and riverine formations. The occurrence of these formations at intermediate depth is also less common. However, their presence cannot be ignored especially in the central and northern Netherlands (Appendix 5). It should be realised that DT refers to the ice-pushed deposits which are commonly riverine or marine sediments; the Urk Formation is among the most important formations being ice-pushed. Geochemically, these sediments may thus be similar to the riverine or marine sediments when their palaeohydrological evolution has also been comparable. The heterogeneity of this unit is to some extent reflected in the scatter of the samples in the Ca carbonate content versus clay content plot (Figure 3.8)

The averages and standard deviations of the primary reaction capacity variables are presented in Table 3.8 for sand and clay in the other formations. The reactivity of clay is larger than of sand, like for the marine and riverine formations. The average contents for Ca carbonate are overall lower than for riverine or marine formations, for organic matter it is comparable to the marine formations and for clay comparable to the riverine formations. Too few data are available for the other three variables in order to enable a meaningful comparison: only 22 Peelo samples from two drillings. The correlation coefficients between clay content and the other primary reaction capacity variables are in most cases high with most values above 0.7 (Table 3.9). This is also clear from the scatter plots (Figure 3.8), which show that these correlations are also meaningful. One should note the two subgroups in the Peelo Formation that can be recognised based on clay content: one sandy group (clay content mostly below 8%) and one clayey group (clay content mostly between 20-30%). For this formation, the correlation coefficient between organic matter and pyrite is 0.684 so the two variables are to some extent related to each other. For Fe and S, it holds that pyrite and reactive Fe occur frequently together (Figure 3.9) and elemental S was near-zero. So, there is sufficiently reactive Fe present to bind all reduced S for this limited series of samples. It cannot be assured that this is a general truth for the Peelo Formation.

Table 3.8. Average contents with related standard deviations (in wt%) of the primary geochemical variables in the other geological formations as present at intermediate depth.

Formation	clay	Ca-carbonate	org. matter	pyrite	reactive Fe	elemental S
sand						
PE	4.2 ± 2.8	1.3 ± 1.7	0.6 ± 0.8	0.2 ± 0.3	1.2 ± 3.1	0 ± 0
BX	1.0 ± 2.0	0.9 ± 2.9	1.4 ± 2.3			
DT	1.1 ± 1.9	0.8 ± 1.5			0 ± 0	
clay						
PE	20.4 ± 8.5	5.8 ± 4.6	2.6 ± 1.5			
BX	16.2 ± 5.4	2.0 ± 0.7	3.2 ± 2.8			
DT	17.4 ± 5.8	10.2 ± 6.1	0.5 ± 0.6			

Table 3.9. Correlation coefficient between clay content and other primary reaction capacity variables for the other formations.

ALL (n = 161)	Ca carbonate	org. matter	pyrite	reactive Fe	elemental S
PE	0.857	0.792	0.921	0.086	0.921
BX	0.357	0.304			
DT	0.727				

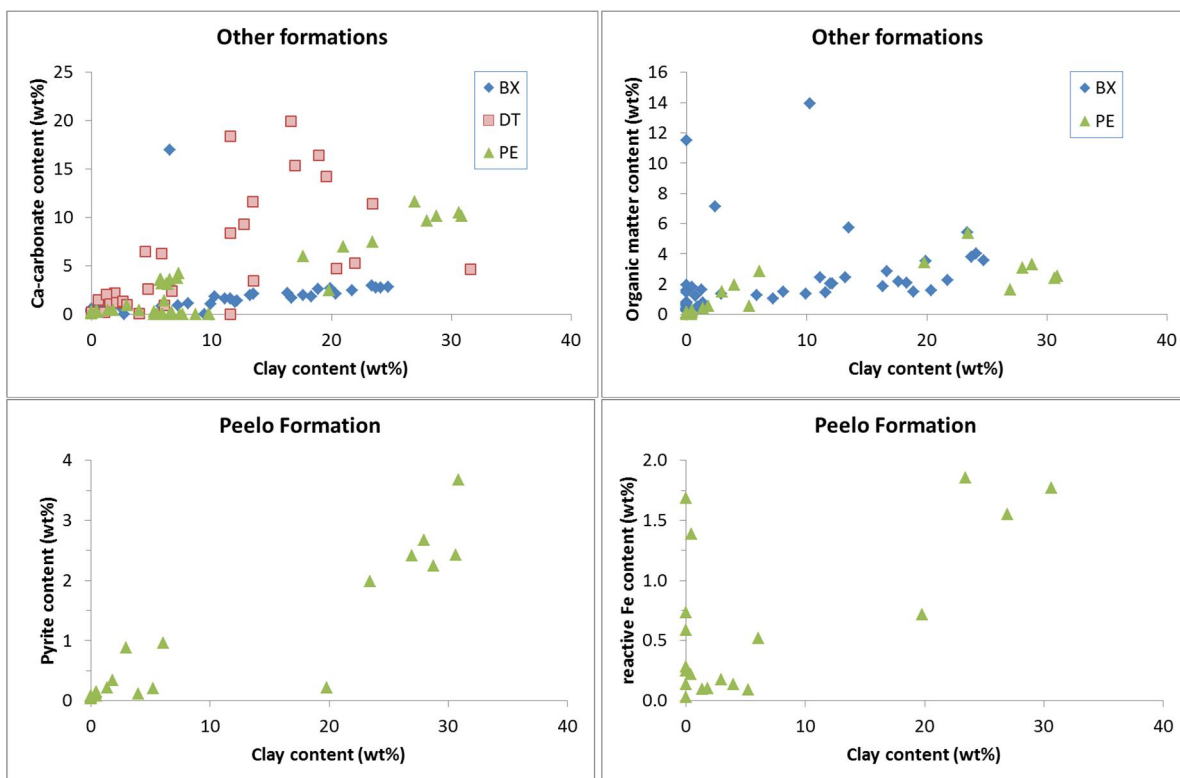


Figure 3.8. Scatter plots between clay content and the other primary reaction capacity variables for the other formations.

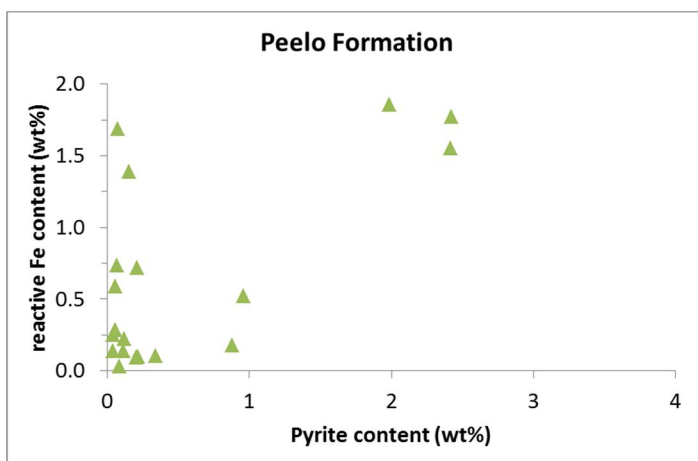


Figure 3.9. Scatter plot between pyrite and reactive Fe for a small series of samples present from the Peelo Formation.

3.3 Secondary reaction capacity variables

The previous section addressed the primary reaction capacity variables. Now, we will address CEC and CBPO as secondary reaction capacity variables. These two variables are interesting within the framework of subsurface disposal of radioactive waste. CEC is relevant as it indicates the sorption capacity for cations and it also provides an indicator for the sorption capacity of anions although clay content is a better, more direct indicator for the anion exchange capacity of clay minerals. CBPO is of importance with respect to the vulnerability of the subsurface for acidification upon pyrite oxidation at the geological scale. Glacial erosion might remove large masses of sediments forming subglacial tunnel valleys and enhanced exposure of the presently buried sediments to air might happen. Associatedly, pyrite oxidation might become an active process as it now happens in soils of reclaimed polders, etc.

The relevant statistics are presented in Appendix 6 organised according to the sedimentary environment of the geological formations. Table 3.10 presents a summary of some of the statistics. Averages are presented for CEC because the average capacity is most relevant at large spatial scale. The average CEC varies within a factor of 2 for clay and varies much more for sand. The related graph in Figure 3.10 indicates that CEC is strongly linearly related with clay content for the clayey samples (note that CEC is directly dependent on clay content and not an independent variable). This means that the variation in organic matter content is of small importance. Several clay samples lie markedly above the linear relationship which are samples rich in organic matter. Most of these samples are riverine. For sand with clay content < 2.5 wt%, CEC values up to 25 meq/kg are not uncommon, which indicates that the organic matter contributes strongly to the CEC in such samples.

Table 3.10. Average CECs (in meq/kg) and two percentile values of CBPO (in mmol/kg) for sand and clay in various geological formations that are found at intermediate depth.

Formation	average CEC	p17.5 CBPO	p82.5 CBPO	average CEC	p17.5 CBPO	p82.5 CBPO
	sand			clay		
	marine formations					
RU				106		
N	39.4			73.5		
BR	21.2	6.3	48.6	156	20.9	215
OO	12.1	-34.4	13.7	125	-105	439
	riverine formations					
AP	2.2	-11.3	8.4			
URTY	23			129		
SY				149	-89.4	25.4
ST	15	21.3	681	102	1200	1855
PZWA	8.5	1.8	18.1	127	102	1890
	other formations					
PE	15.4	-6.5	16.6			
BX	25.3			131		

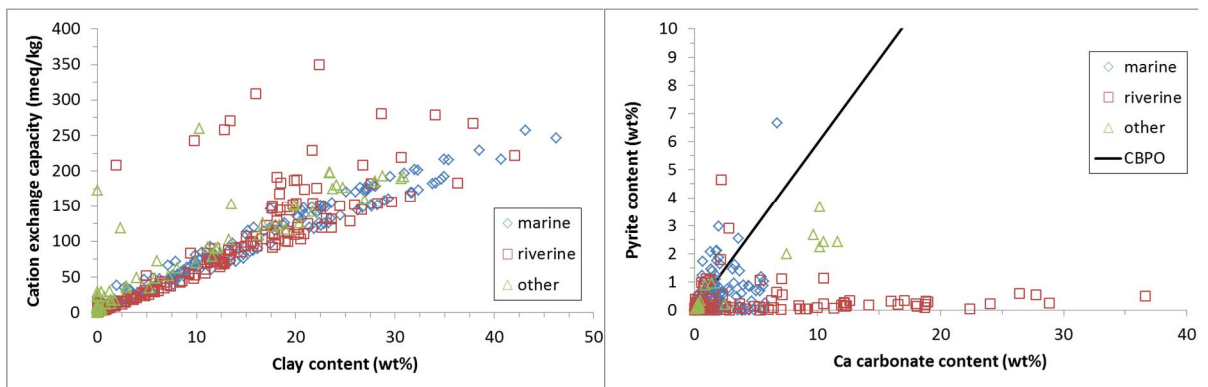


Figure 3.10. Scatter plots for all relevant samples of the CEC versus clay content (left) and the pyrite versus Ca carbonate content (right). The line indicates the stoichiometric relation for CBPO where all samples to the right have a Ca carbonate excess and those above a deficit.

In Table 3.10, the 17.5 and 82.5 percentiles are presented for CBPO in order to indicate the vulnerability for acidification: negative values indicate vulnerable for acidification, i.e., a stoichiometric excess of pyrite versus Ca-carbonate. Figure 3.10 also presents a graph that indicates the distribution of samples that are well pH-buffered for oxidation and those that are not. The data indicate that the 17.5 percentile is negative for some formations, where more negative values are found for clay than for sand. This implies that a substantial amount of samples has a deficit in carbonate buffering upon pyrite oxidation. Oppositely, a large group of riverine samples has a high carbonate content and pyrite content below 1%, which are thus extremely well buffered.

4 Conclusions

Existing data sets of geochemical analysis of the subsurface were set in one Access database. The samples were classified on lithological class and geological formation. Samples deeper than 30 m depth were selected for further statistical characterisation. A total of 2700 samples were obtained in this way that are associated with 15 geological formations (where two members were individually considered for one formation).

The characterisation procedure for reaction capacities of geological units that was established by TNO Geological Survey, was applied to the data. The primary reaction capacity variables clay, Ca carbonate, pyrite, non-pyrite reactive Fe and elemental S were derived from the geochemical analyses together with the secondary reaction capacity variables cation-exchange capacity (CEC), total reduction capacity and carbonate buffering following acidification upon pyrite oxidation (CBPO). The secondary variables were calculated by combining two primary variables. The characterisation obtained must be considered as preliminary because no rigorous quality control was performed on the data. However, the impression is that the results are overall reliable and the statistical index numbers obtained are useful at the national scale. The obtained national characterisation of the subsurface at intermediate depth (30-400 m) is novel for the Netherlands.

As expected, clay has higher averages in reaction capacities than sand. An exception may be reactive Fe that can be higher in marine sand probably due to more SO_4 -reducing conditions in marine clay than sand. Marine sand is more reactive than riverine sand. Few data was available for formations other than marine or riverine ones in particular on pyrite, reactive Fe and elemental S. Correlation coefficients among the primary reaction capacity variables (as absolute values) are generally below 0.7, which implies that one variable cannot be reliably estimated from another variable. With respect to the secondary reaction capacity variables, CEC of clay is majorly controlled by clay content and not organic matter content and CBPO is generally positive (i.e., sediment is well-buffered against acidification upon pyrite oxidation). The obtained statistical index numbers can be used for groundwater transport simulations and other purposes.

5 References

- Bakker, I., Kiden, P., Schokker, J. & Griffioen, J. (2007). De GeoTOP van de ondergrond: Een reactievat. Deelrapport 2. Eerste statistische karakterisatie van de geochemische reactiecapaciteit van het topsysteem in Noord-Brabant en het noorden van Limburg. TNO Bouw en Ondergrond, rapportno. 2007-U-R0324/A.
- Bates, A.L., Spiker, E.C. and Holmes, C.W. (1998). Speciation and isotopic composition of sedimentary sulfur in the Everglades, Florida, USA. *Chem. Geol.* (146), 155-170.
- Bosch, J.H.A., Harting, R. & Gunnink, J. (2014). Lithologische karakterisering van de ondiepe ondergrond van Noord-Nederland (Topsysteem hoofdgebied 5). TNO-Geologische Dienst Nederland, rapportno. 2014-R10680, 94 p + bijlagen.,
- Broers, H.P. (2002). Strategies for regional groundwater quality monitoring. Ph.D thesis, University Utrecht, 231 pp.
- Chambers, R.M. and Pederson, K.A. (2006). Variation in soil phosphorus, sulfur, and iron pools among south Florida wetlands. *Hydrobiologia* (569), 63-70.
- Fest, E.P.M.J., Temminghoff, E.J.M., Griffioen, J., Van der Grift, B. & Van Riemsdijk, W.H. (2007). Groundwater chemistry of Al under Dutch acid sandy soils: effects of land use and depth. *Appl. Geochem* (22), 1427-1438.
- Griffioen, J., Klein, J. & Van Gaans, P.F.M. (2012). Reaction capacity characterisation of shallow sedimentary deposits in geologically different regions of the Netherlands. *J. Cont. Hydrol* (127), 30-46.
- Griffioen, J., Vermooten, S. & Janssen, G.J.A. (2013). Geochemical and palaeohydrological controls on the composition of shallow groundwater in the Netherlands. *Applied Geochem.* (39), 129-149. Doi: 10.1016/j.apgeochem.2013.10.005
- Griffioen, J., Klaver, G. & Westerhoff, W. (2016). The mineralogy of suspended matter, fresh and Cenozoic sediments in the fluvio-deltaic Rhine-Meuse-Scheldt-Ems area, the Netherlands: An overview and review. *Neth. J. Geosci.*, in press.
- Groenendijk, P., Renaud, L.V., Roelsma, J., Janssen, G., Jansen, S., Heerdink, R., Griffioen, J. & Van der Grift, B. (2008). Compliance checking level of nitrate in groundwater. Investigations of lowering the depth to 5 m below the phreatic surface with a regional leaching model. Alterra, Deltares.
- Hartog, N., Griffioen, J. & Van der Weijden, C.H. (2002). Distribution and reactivity of O₂-reducing components in sediments from a layered aquifer. *Env. Science & Technol.* (36), 2338-2344.
- Hartog, N., Griffioen, J. & Van Bergen, P.F. (2005). Depositional and paleohydrogeological controls on the reactivity of organic matter and other reductants in aquifer sediments. *Chem. Geol.* (216), 113-131.
- Heerdink, R. & Griffioen, J. (2008). Methodeontwikkeling voor het berekenen van het gehalte reactief ijzer uit totaalgehalten ijzer en aluminium in sediment. TNO/Deltares, 2008-U-R1278/A.
- Heerdink, R. (2009). Regionale geochemische karakterisering van de Nederlandse ondergrond binnen TOPINTEGRAAL: de statistische methodes. TNO Bouw en Ondergrond, rapportno. 0910-0011.
- Heerdink, R. & Griffioen, J. (2012). Geochemische karakterisering van de geotop van Noord-Nederland (hoofdgebied 5). Gehaltes en associaties van hoofd- en sporenelementen. TNO Energie, rapportno. TNO2012R10136, 227 pp.
- Huisman, D.J. & Kiden, P. (1998). A geochemical record of Late Cenozoic sedimentation history in the southern Netherlands. *Geologie en Mijnbouw* (76), 277-292.

- Jakobsen, R. & Cold, L. (2007). Geochemistry at the sulfate reduction – methanogenesis transition zone in an anoxic aquifer – A partial equilibrium interpretation using 2D reactive transport modeling. *Geochim. Cosmochim. Acta* (71), 1949-1966.
- Klein, J. & Griffioen, J. (2008). Het topsysteem van de ondergrond: Een reactievat. Deelrapport 8. Pilot-studie naar de reactiecapaciteit van twee geologische formaties in Noord-Brabant. TNO-Alterra Rapport 2008-U-R0797/A.
- Klein, J. & Griffioen, J. (2012). Geochemische karakterisering van de GeoTOP van Noord-Nederland (hoofdgebied 5). De reactiecapaciteit van afzettingen in de GeoTOP van Noord-Nederland. TNO geological Survey of the Netherlands, rapportno. TNO-034-UT-2010-01286, 165 pp.
- Klein, J., Van Gaans, P. & Griffioen, J. (2015). Geochemische karakterisering van de geotop van Holland (gebied 1b en 1c). TNO, rapportno. TNO 2015 R 10785, 419 pp.
- Koenen, M. & Griffioen J. (2014). Geochemical characterisation of the Boom Clay. Report OPERA-PU-TNO521-1, 103 pp.
- Massmann, G., Pekdeger, A. & Merz, C. (2004). Redox processes in the Oderbruch polder groundwater flow system in Germany. *Appl. Geochem.* (19), 863-886.
- Ritsema, C.J. & Groenenberg, J.E. (1993). Pyrite oxidation, carbonate weathering, and gypsum formation in a drained potential acid sulfate soil. *Soil Sci. Soc. Am. J.* (57), 968-976.
- Schwientek, M., Einsiedl, F., Stichler, W., Stoegbauer, A., Strauss, H. & Maloszewski, P. (2008). Evidence for denitrification regulated by pyrite oxidation in a heterogeneous porous groundwater system. *Chem. Geol.* (255), 60-67.
- Van Gaans, P.F.M., Griffioen, J., Mol, G., Klaver, G.T. (2011). Geochemical reactivity of subsurface sediments as potential buffer to anthropogenic inputs: a strategy for regional characterization in the Netherlands. *J. Soils Sed.* (11), 336-351. DOI 10.1007/s11368-010-0313-4.
- Van Helvoort, P.J. (2003). Complex confining layers. A physical and geochemical characterization of heterogeneous unconsolidated fluvial deposits using a facies-based approach. Ph.D thesis, Utrecht University, 147 pp.
- Van Helvoort, P.J., Griffioen, J. & Hartog, N. (2007). Characterization of the reactivity of riverine heterogeneous sediments using a facies-based approach: The Rhine-Meuse delta (the Netherlands). *Appl. Geochem* (22), 2735-2757.
- Vermooten, S., Griffioen, J., Heerdink, R. & Visser, A. (2011). Geochemische karakterisering van de GeoTOP van Zeeland. TNO, rapport no. TNO-034-UT-2010-02397, 138 pp.

A Data sources

Source	FromSubTable	FromTable	Count	Copied	Location original file
ACME analyses	Huisman	Maalbeek	52	52	...\Maalbeek-groeve_ACME-analyses.xlsx
GC	Huisman	GC_Kempen	130	130	...\GC_diepe bo Kempen.xls
GC	Huisman	GC_Schokker	153	117	...\GC_bo Schokker.xls
Gunnink	Gunnink	Gunnink	6265	1785	...\opslag Geoch analyses\TNO-projecten\XRF_JanGunnink.xls
Huisman	Huisman	Huisman	4962	4851	...\Alle_XRF_gegevens_NITG_nw_Huisman.zip
Sed.anal. KWR Suyfzand	KWR	KWR_WOG1	x	0	...\sedimentanalyses-KWR-Stuyfzand\WOG t Klooster - Gelderland.xlsx
Sed.anal. KWR Suyfzand	KWR	WKR_WOG2	49	49	...\sedimentanalyses-KWR-Stuyfzand\chemischeAnalyses-WOG-tKlooster-Gelderland.xlsx
Sed.anal. KWR Suyfzand	KWR	KWR_Someren	14	12	...\sedimentanalyses-KWR-Stuyfzand\Chemische samenstelling van boven miocene zandmonsters uit boring 51H.171 te Someren in relatie tot diepinfiltratie (DIZON)\
Sed.anal. KWR Suyfzand	KWR	KWR_Roosteren	45	45	...\sedimentanalyses-KWR-Stuyfzand\Chemische samenstelling van het eerste ...in relatie tot Maasoeverfiltratie\
Sed.anal. KWR Suyfzand	KWR	KWR_WW_T41	15	15	...\sedimentanalyses-KWR-Stuyfzand\Chemische samenstelling van zandmonsters uit 3 waterwingebieden\
Sed.anal. KWR Suyfzand	KWR	KWR_WW_T42	15	15	...\sedimentanalyses-KWR-Stuyfzand\Chemische samenstelling van zandmonsters uit 3 waterwingebieden\
Sed.anal. KWR Suyfzand	KWR	KWR_WW_T45	53	52	...\sedimentanalyses-KWR-Stuyfzand\Chemische samenstelling van zandmonsters uit 3 waterwingebieden\
CAL-GT-02	Huisman	CAL-GT-02	76	76	...\sedimentanalyses_CAL-GT-02.xlsx
CAL-GT-02_xrd_clay	Huisman	CAL-GT-02_xrd_clay	6	6	...\sedimentanalyses_CAL-GT-02.xlsx
CAL-GT-02_bulk	Huisman	CAL-GT-02_bulk	6	6	...\sedimentanalyses_CAL-GT-02.xlsx
TNO-proj. - data v. STONE	Huisman	STONE_BVGB_Veghel	75	0	...\opslag Geoch analyses\TNO-projecten\data tbv STONE\brabantveghelgemertbudel.xls
TNO-proj. - data v. STONE	Huisman	STONE_BVGB_Budel	35	0	...\opslag Geoch analyses\TNO-projecten\data tbv STONE\brabantveghelgemertbudel.xls
TNO-proj. - data v. STONE	Huisman	STONE_BVGB_Gemert	106	106	...\opslag Geoch analyses\TNO-projecten\data tbv STONE\brabantveghelgemertbudel.xls
TNO-proj. - data v. STONE	Huisman	STONE_HO_SED_507	10	10	...\opslag Geoch analyses\TNO-projecten\data tbv STONE\heumensoord_sedimentanalyses.xls

Source	FromSubTable	FromTable	Count	Copied	Location_original file
TNO-proj. - data v. STONE	Huisman	STONE_HO_SED_506	13	13	... \opslag_Geoch_analyses\TNO-projecten\data tbv STONE\heumensoord_sedimentanalyses.xls
TNO-proj. - data v. STONE	Huisman	STONE_Kempen	x	x	... \opslag_Geoch_analyses\TNO-projecten\data tbv STONE\kempen.xls
TNO-proj. - data v. STONE	STONE	STONE_Adam		0	... \opslag_Geoch_analyses\TNO-projecten\data tbv STONE\amsterdamarseenxrf.xls
TNO-proj. - data v. STONE	STONE	STONE_NM	74	0	... \opslag_Geoch_analyses\TNO-projecten\data tbv STONE\nulandmacharen.xls
TNO-proj. - data v. STONE	STONE	- Parond2	344	0	... \opslag_Geoch_analyses\TNO-projecten\data tbv STONE\parond2.xls
TNO-proj. - data v. STONE	STONE	- Parond3	78	0	... \opslag_Geoch_analyses\TNO-projecten\data tbv STONE\parond3.xls
TNO-proj. - data v. STONE	STONE	- Parond4	168	0	... \opslag_Geoch_analyses\TNO-projecten\data tbv STONE\parond4.xls
TNO-proj. - data v. STONE	STONE	- Parond5	154	0	... \opslag_Geoch_analyses\TNO-projecten\data tbv STONE\parond5.xls
TNO-proj. - data v. STONE	STONE	- Parond_geokar	18	18	... \opslag_Geoch_analyses\TNO-projecten\data tbv STONE\parond geokar.xls
TNO-proj. - data v. STONE	STONE	- Parond_Vecht1	143	0	... \opslag_Geoch_analyses\TNO-projecten\data tbv STONE\parond vechtstreek - arseen.xls
TNO-proj. - data v. STONE	STONE	- Parond_Vecht2	84	0	... \opslag_Geoch_analyses\TNO-projecten\data tbv STONE\parond vechtstreek - arseen II.xls
TNO-proj. - data v. STONE	STONE	STONE_TX_tga	181	0	... \opslag_Geoch_analyses\TNO-projecten\data tbv STONE\texeltga.xls e.a. texel
TNO-proj. - data v. STONE	STONE	STONE_TX_xrf	55	0	... \opslag_Geoch_analyses\TNO-projecten\data tbv STONE\texeltga.xls e.a. texel
Wubben	STONE	Zeeuwsvlaanderen	286	146	... \L Wubben\Klaar om in te voeren\NOG niet geschikt voor loader\Zeeuws_Vlaanderen\
Wubben	Wubben	Wubben_V	0	0	... \L Wubben\Klaar om in te voeren\Korrel grootte\
Wubben	Wubben	Wubben_Kempen	0	0	... \L Wubben\NIET INVOEREN\Kempen\
Wubben	Wubben	Buizen Interreg	67	67	... \L Wubben\Klaar om in te voeren\NOG niet geschikt voor loader\BUIZEN nog niet bekend\Restant_data_Interreg\LW_Rest_Data_Interreg_onbekend27-3-2007.xls
Wubben	Wubben	Buizen_LUW	25	25	... \L Wubben\Klaar om in te voeren\NOG niet geschikt voor loader\BUIZEN nog niet bekend\LUW\rvR_LUW_06-11-06.xls
Wubben	Wubben	GR_BI_Slinger	17	16	... \L Wubben\Klaar om in te voeren\NOG niet geschikt voor loader\Groen blauwe slinger\LW_Gr_BI_Slinger_04-01-07.xls
Wubben	Wubben	LW_Texel	236	181	... \L Wubben\Klaar om in te voeren\NOG niet geschikt voor loader\Texel\LW_Texel_04-01-07.xls
Wubben	Wubben	Nuland_Marc haren	74	74	... \L Wubben\Klaar om in te voeren\NOG niet geschikt voor

Source	FromSubTable	FromTable	Count	Copied	Location_original file
					loader\Nuland_Marcharen\LW_Nuland-Marcharen_03-01-07.xls
Wubben	Wubben	PMG_Brabant	502	502	...\L Wubben\Klaar om in te voeren\NOG niet geschikt voor loader\PMG_Brabant\AB_PMG_Brabant_08-11-06.xls
Wubben	Wubben	RIVM_Denit	151	132	...\L Wubben\Klaar om in te voeren\NOG niet geschikt voor loader\RIVM_Denitrificatie_2005\LW_RIVM_denitrificatie_04-01-07.xls
Wubben	KWR	Holten	18	18	...\L Wubben\Klaar om in te voeren\NOG niet geschikt voor loader\Holten-sediment\LW_Bodem_Holten-sediment_04-01-07.xls
Wubben	Wubben_Parond	Amsterdam_As	137	95	...\L Wubben\Klaar om in te voeren\NOG niet geschikt voor loader\Amsterdam_Arseen\LW_Amsterdam_Arseen_15-3-07.xls
Wubben	Wubben_Parond	Gemert	106	45	...\L Wubben\Klaar om in te voeren\NOG niet geschikt voor loader\Gemert\LW_Gemert_3-01-07.xls
Wubben	Wubben_Parond	Heumensoord	23	23	...\L Wubben\Klaar om in te voeren\NOG niet geschikt voor loader\Heumensoord\LW_Origineel_Heumensoord_04-01-07.xls
Wubben	Wubben_Parond	Hilvarenbeek	156	156	...\L Wubben\Klaar om in te voeren\NOG niet geschikt voor loader\Hilvarenbeek\LW_Hilvarenbeek_03-01-07.xls
Wubben	Wubben_Parond	Noordbargeres	75	75	...\L Wubben\Klaar om in te voeren\NOG niet geschikt voor loader\Noordbargeres\RvR_Noordbargeres_08-11-06.xls
Wubben	Wubben_Parond	Parond_Vecht_As	227	227	...\L Wubben\Klaar om in te voeren\NOG niet geschikt voor loader\Parond_Vechtstreek_Arseen\LW-Parond_Vecht_Arseen_04-01-07.xls
Wubben	Wubben_Parond	Parond1	140	140	...\L Wubben\Klaar om in te voeren\NOG niet geschikt voor loader\Parond1\LW_Parond1_04-01-07.xls
Wubben	Wubben_Parond	Parond2	344	344	...\L Wubben\Klaar om in te voeren\NOG niet geschikt voor loader\Parond2\LW_Parond2_04-01-07.xls
Wubben	Wubben_Parond	Parond3	78	78	...\L Wubben\Klaar om in te voeren\NOG niet geschikt voor loader\Parond3\LW_Parond3_04-01-07.xls
Wubben	Wubben_Parond	Parond4	168	168	...\L Wubben\Klaar om in te voeren\NOG niet geschikt voor loader\Parond4\RvR_Parond4_08-11-06.xls

<u>Source</u>	<u>FromSubTable</u>	<u>FromTable</u>	<u>Count</u>	<u>Copied</u>	<u>Location_original file</u>
Wubben	Wubben_Parond	Parond5	154	154	...\L Wubben\Klaar om in te voeren\NOG niet geschikt voor loader\Parond5\LW_Parond5_04-01-07.xls

B Criteria per formation for different ranges in Al₂O₃ contents

Formation Name		Al ₂ O ₃ <5%		Al ₂ O ₃ >5%		Type
		intercept	slope	intercept	slope	
AP	Appelscha	-0.18	0.13	-1	0.4	Riverine
BE	Beegden	-0.18	0.13	-1	0.4	Other Formations
BR	Breda	-0.6	0.32	-1	0.4	Marine
BX	Boxtel	-0.18	0.13	-0.6	0.24	Other Formations
DN	Drachten	-0.18	0.13	-0.6	0.24	Other Formations
DO	Dongen	-0.6	0.32	-1	0.4	Marine
DR	Drente	-0.18	0.13	-0.6	0.3	Glacial / Other Formations
DT	gestuwd (ice-pushed)	-0.18	0.13	-1	0.4	Other Formations
EE	Eem	-0.6	0.32	-0.6	0.3	Marine
HL	Holoceen	-0.6	0.32	-1	0.4	
KI	Kiezeloolliet	-0.18	0.13	-1	0.4	Riverine
KR	Kreftenheye	-0.18	0.13	-1	0.4	Riverine
MS	Maassluis	-0.6	0.32	-1	0.4	Marine
N	Basis Noordzee Groep	-0.6	0.32	-1	0.4	Base of the North Sea Group
OO	Oosterhout	-0.6	0.32	-1	0.4	Marine
PE	Peelo	-0.18	0.13	-0.6	0.24	Other Formations
PZWA	Peize/Waalre	-0.18	0.13	-1	0.4	Riverine
RU	Rupel	-0.6	0.32	-1	0.4	Marine
ST	Sterksel	-0.18	0.13	-0.6	0.24	Riverine
SY	Stramproy	-0.18	0.13	-0.6	0.24	Riverine
TO	Tongeren	-0.6	0.32	-1	0.4	Marine
URTY	Urk, Tijnje Member	-0.18	0.13	-1.75	0.4	Riverine
URVE	Urk, Veenhuizen Member	-0.18	0.13	-1.75	0.4	Riverine

C VBA code to edit detection-limits of elements

```

Sub ChngQRY()

Dim strsql As Variant
Dim qdf As QueryDef
Dim sqlString As String
Dim Elements As Variant

DoCmd.SetWarnings False

Elements = Array("SiO2", "Al2O3", "TiO2", "Fe2O3", "MnO", "CaO", "MgO", "Na2O", "K2O", "P2O5", "S",
"Sum", "As", "Cu", "Pb", "Zn", "Ni", "Cr", "V", "Sn", "Sr", "Ba", "Rb", "Ga", "Zr", "Nb", "Y", "Sc",
"La", "Nd", "Th", "U", "Totaal C", "TOC", "S (%)", "Li", "Be", "Na", "Mg", "Al", "P", "K", "Ca", "Ti",
"Mn", "Fe", "Co", "Se", "Mo", "Ag", "Au", "Cd", "Sb", "Te", "Cs", "Ce", "Pr", "Sm", "Eu", "Gd", "Tb",
"Dy", "Ho", "Er", "Tm", "Yb", "Lu", "Hf", "Ta", "W", "Hg", "Tl", "Bi")
' Elements = Array("SiO2", "Al2O3", "TiO2", "MnO")

' replace SQL string
Set db = CurrentDb()
Set qdf = db.QueryDefs("NewQuery")

For Each El In Elements
    sqlString = "UPDATE basis SET basis.[" & El & "] = -0.5*[" & El & "], basis.[dl_" & El & "] = '<' &
[" & El & "] " & _
    "WHERE (((basis.[" & El & "])<0));"
    qdf.SQL = sqlString
    ' Run qry
    DoCmd.OpenQuery qdf.Name
    Debug.Print sqlString
Next El

DoCmd.SetWarnings True

Debug.Print "done"

End Sub

```


D SQL queries for calculating reactive capacities and selecting the data > 30m deep

```

001_mkt_basis_recap SELECT basis.ID AS Basis_ID, basis.[X coördinaat], basis.[Y coördinaat], basis.BORING, basis.FromTable, basis.Mid,
basis.LocDepth_ID, basis.maaiveld, basis.diepte, basis.[formatie (HvdM)], basis.Formatie, basis.[Totaal C], basis.TOC, basis.S, basis.[S
(%)], basis.AI, basis.CaO, basis.Ca, basis.Al2O3, basis.Fe, basis.Fe2O3, basis.ZKV, noexec_myZKL.ZKL, basis.[Org C %], basis.[TGA
105-450], basis.[TGA 450-550], basis.[TGA 550-800], basis.[TGA 800-1000], basis.lutum, noexec_myZKL.silt, noexec_myZKL.sand
INTO basis_recap FROM basis INNER JOIN noexec_myZKL ON basis.ID = noexec_myZKL.ID;

001b_addfields ALTER TABLE basis_recap ADD ZKV_new TEXT, gtst5 TEXT, intercept DOUBLE, slope DOUBLE, AI_use DOUBLE, Fe_use DOUBLE,
S_use DOUBLE, Ca_use DOUBLE, Pyriet_obvS DOUBLE, Niet_reacFe double, ReacFe double, Fe_Pyriet_obvS double,
Fe_Pyriet_obvS_cor double, Fe_reac double, S_Pyriet double, Pyriet double, S_org double, S_gedegen double, OS_TOC double,
OS_TGA double, OS double, Carbonaat double, PRC DOUBLE, CEC DOUBLE, CPBO DOUBLE, ZKVFormatie TEXT 001c_fill_basic
UPDATE basis_recap SET basis_recap.AI_use = [Al2O3], basis_recap.Fe_use = [Fe2O3], basis_recap.S_use = [S (%)],
basis_recap.Ca_use = [CaO];

001d_fill_AI UPDATE basis_recap SET basis_recap.AI_use = [Al] WHERE (((basis_recap.AI_use) Is Null) AND ((basis_recap.AI)<1000));

001d_fill_Ca UPDATE basis_recap SET basis_recap.Ca_use = [Ca] WHERE (((basis_recap.Ca_use) Is Null));

001d_fill_Fe UPDATE basis_recap SET basis_recap.Fe_use = [Fe] WHERE (((basis_recap.Fe_use) Is Null) AND ((basis_recap.Fe)<1000));

001d_fill_S UPDATE basis_recap SET basis_recap.S_use = [S] WHERE (((basis_recap.S_use) Is Null) AND ((basis_recap.S)<1000));

001e_calc_lutum UPDATE basis_recap SET basis_recap.lutum = 1.96*[Al2O3]-2.36 WHERE (((basis_recap.lutum) Is Null) AND ((basis_recap.AI_use) Is
Not Null));

001e_TGA450 UPDATE basis_recap SET basis_recap.[TGA 105-450] = -0.5*[TGA 105-450] WHERE (((basis_recap.[TGA 105-450])<0));

001f_lutum_st0 UPDATE basis_recap SET basis_recap.lutum = 0 WHERE (((basis_recap.lutum)<0));

001f_TGA550 UPDATE basis_recap SET basis_recap.[TGA 550-800] = -0.5*[TGA 550-800] WHERE (((basis_recap.[TGA 550-800])<0));

001g_TGA800 UPDATE basis_recap SET basis_recap.[TGA 800-1000] = -0.5*[TGA 800-1000] WHERE (((basis_recap.[TGA 800-1000])<0));

001h_TGA450 UPDATE basis_recap SET basis_recap.[TGA 450-550] = -0.5*[TGA 450-550] WHERE (((basis_recap.[TGA 450-550])<0));

002_set_ZKL UPDATE basis_recap SET basis_recap.ZKV_new = [ZKL] WHERE (((basis_recap.ZKV_new) Is Null) AND ((basis_recap.ZKL) Is Not
Null));

002a_ZKVrest UPDATE basis_recap SET basis_recap.ZKV_new = If([lutum]<8,"Z","K") WHERE (((basis_recap.ZKV_new) Is Null));

002b_set_K UPDATE basis_recap SET basis_recap.ZKV_new = "K" WHERE (((basis_recap.ZKV_new) Is Null) AND ((basis_recap.ZKV)="K"));

002c_set_L UPDATE basis_recap SET basis_recap.ZKV_new = "L" WHERE (((basis_recap.ZKV_new) Is Null) AND ((basis_recap.ZKV)="L"));

002d_set_S UPDATE basis_recap SET basis_recap.ZKV_new = "S" WHERE (((basis_recap.ZKV) Like "Schel" Or (basis_recap.ZKV)="She" Or
(basis_recap.ZKV)="schel" Or (basis_recap.ZKV)="S"));

002e_set_V UPDATE basis_recap SET basis_recap.ZKV_new = "V" WHERE (((basis_recap.ZKV_new) Is Null) AND ((basis_recap.ZKV)="V"));

002f_set_Z UPDATE basis_recap SET basis_recap.ZKV_new = "Z" WHERE (((basis_recap.ZKV_new) Is Null) AND ((basis_recap.ZKV)="Z"));

002g_set_Zrest UPDATE basis_recap SET basis_recap.ZKV_new = "Z" WHERE (((basis_recap.ZKV_new) Is Null));

003_OS1_TOC UPDATE basis_recap SET basis_recap.OS_TOC = 2*[TOC], basis_recap.OS = 2*[TOC];

003_OS2_TGA UPDATE basis_recap SET basis_recap.OS_TGA = ((basis_recap)[TGA 105-450]+[basis_recap][TGA 450-550])-
0.07*[basis_recap][lutum];

003_OS3 UPDATE basis_recap SET basis_recap.OS = [OS_TGA] WHERE (((basis_recap.OS) Is Null));

003_OS3_orgC UPDATE basis_recap SET basis_recap.OS = [Org C %] WHERE (((basis_recap.OS) Is Null));

003_OS4_dl UPDATE basis_recap SET basis_recap.OS = -1*[OS] WHERE (((basis_recap.OS)<0));

```

```

003_OS5_VH      SELECT basis_recap.Basis_ID, basis_recap.lutum, basis_recap.silt, basis_recap.sand, basis_recap.OS, 1.047197 AS angle,
                [lutum]+[OS]+[silt]+[sand] AS sumit, [OS]/[sumit]*100 AS OS2, [lutum]/[sumit]*100 AS lutum2, ([sand]+[silt])/[sumit]*100 AS SandSilt,
                [OS2]*Sin([angle]) AS plotY, [plotY]/Tan([angle])+[SandSilt] AS plotX, -0.16762*[SandSilt]+28.49503 AS YV_line,
                If([plotY]>[YV_line],"V","H") AS VH FROM basis_recap;

003_OS6_V      UPDATE basis_recap INNER JOIN 003_OS5_VH ON basis_recap.Basis_ID = [003_OS5_VH].Basis_ID SET basis_recap.ZKV_new =
                "V" WHERE ((([003_OS5_VH].VH)="V"));

004_pyriet_obvS_noV  UPDATE basis_recap SET basis_recap.Pyriet_obvS = (120*[S_use])/(2*32.1) WHERE (((basis_recap.ZKV_new)<>"V") AND
                ((basis_recap.S_use) Is Not Null) AND ((basis_recap.TOC) Is Not Null));

004b_pyriet_obvS_V  UPDATE basis_recap SET basis_recap.Fe_Pyriet_obvS = (120*([S_use]-[OS]/220))/(2*32.1) WHERE (((basis_recap.ZKV_new)="V")
                AND ((basis_recap.S_use) Is Not Null) AND ((basis_recap.TOC) Is Not Null));

005_addCriteria_Intercept TRANSFORM First([Criteria-new_analysis].intercept) AS FirstOfintercept SELECT [Criteria-new_analysis].Formatie FROM [Criteria-
                new_analysis] GROUP BY [Criteria-new_analysis].Formatie PIVOT [Criteria-new_analysis].gtst5;

005_addCriteria_Slope TRANSFORM First([Criteria-new_analysis].slope) AS FirstOfslope SELECT [Criteria-new_analysis].Formatie FROM [Criteria-
                new_analysis] GROUP BY [Criteria-new_analysis].Formatie PIVOT [Criteria-new_analysis].gtst5;

005_gt5         UPDATE basis_recap SET basis_recap.gtst5 = "Al2O3>5%" WHERE (((basis_recap.Al_use)>=5));

005_st5         UPDATE basis_recap SET basis_recap.gtst5 = "Al2O3<5%" WHERE (((basis_recap.Al_use)<5));

005c_addCriteria UPDATE basis_recap INNER JOIN [Criteria-new_analysis] ON (basis_recap.gtst5 = [Criteria-new_analysis].gtst5) AND
                (basis_recap.Formatie = [Criteria-new_analysis].Formatie) SET basis_recap.intercept = [Criteria-new_analysis].[intercept],
                basis_recap.slope = [Criteria-new_analysis].[slope];

006_Niet-Reac_Fe  UPDATE basis_recap SET basis_recap.Niet_reacFe = [slope]*[Al_use]+[intercept];

006_Niet-Reac_Fe_st0 UPDATE basis_recap SET basis_recap.Niet_reacFe = 0 WHERE (((basis_recap.Niet_reacFe)<0));

007_Reac_Fe      UPDATE basis_recap SET basis_recap.ReacFe = (2*55.58*([Fe_use]-[Niet_reacFe]))/(2*55.85+48);

007_Reac_Fe_st0  UPDATE basis_recap SET basis_recap.ReacFe = 0 WHERE (((basis_recap.ReacFe)<0));

008_Fe_Pyriet_obvS  UPDATE basis_recap SET basis_recap.Fe_Pyriet_obvS = 55.85*[Pyriet_obvS]/(2*32.1+55.85);

009_Fe_Pyriet_obvS_cor UPDATE basis_recap SET basis_recap.Fe_Pyriet_obvS_cor = [ReacFe] WHERE (((basis_recap.Fe_Pyriet_obvS)>=[ReacFe]));

009_Fe_Pyriet_obvS_cor_stFe  UPDATE basis_recap SET basis_recap.Fe_Pyriet_obvS_cor = [Fe_Pyriet_obvS] WHERE
                (((basis_recap.Fe_Pyriet_obvS)<[ReacFe]));

010_Fe_reac_gt0   UPDATE basis_recap SET basis_recap.Fe_reac = [ReacFe]-[Fe_Pyriet_obvS_cor] WHERE (((basis_recap.ReacFe)>0));

010_Fe_reac_st0   UPDATE basis_recap SET basis_recap.Fe_reac = 0 WHERE (((basis_recap.ReacFe)=0));

011_S_Pyriet      UPDATE basis_recap SET basis_recap.S_Pyriet = [Fe_Pyriet_obvS_cor]*64.2/55.85;

012_Pyriet_noV    UPDATE basis_recap SET basis_recap.Pyriet = [S_Pyriet]*120/(2*32.1) WHERE (((basis_recap.ZKV_new)<>"V"));

012_Pyriet_V_gt0  UPDATE basis_recap SET basis_recap.Pyriet = ([S_Pyriet]-([OS]/220)) WHERE (((basis_recap.ZKV_new)="V"));

012_Pyriet_V_st0  UPDATE basis_recap SET basis_recap.Pyriet = 0 WHERE (((basis_recap.Pyriet)<=0) AND ((basis_recap.ZKV_new)="V"));

012_Pyriet_V_zcalc UPDATE basis_recap SET basis_recap.Pyriet = [Pyriet]*120/(2*32.1) WHERE (((basis_recap.ZKV_new)="V"));

013_Sorg_noV      UPDATE basis_recap SET basis_recap.S_org = 0 WHERE (((basis_recap.ZKV_new)<>"V"));

013_Sorg_V1       UPDATE basis_recap SET basis_recap.S_org = [OS]/220 WHERE (((basis_recap.ZKV_new)="V"));

013_Sorg_V2       UPDATE basis_recap SET basis_recap.S_org = [S_use] WHERE (((basis_recap.S_org)>[S_use]));

014_Sgedegen      UPDATE basis_recap SET basis_recap.S_gedegen = [S_use]-[S_Pyriet]-[S_org];

015_Carbonaat     UPDATE basis_recap SET basis_recap.Carbonaat = [TGA 550-800]*100/44;

015b_Carbonaat_CaO UPDATE basis_recap SET basis_recap.Carbonaat = 100/56.0774*([Ca_use]-0.0448*[Al_use]-0.1147) WHERE (((basis_recap.Ca_use)
                Is Not Null) AND ((basis_recap.Al_use) Is Not Null) AND ((basis_recap.Carbonaat) Is Not Null));

015c_Carbonaat_st0 UPDATE basis_recap SET basis_recap.Carbonaat = 0 WHERE (((basis_recap.Carbonaat)<0));

```

```

016_PRC          UPDATE basis_recap SET basis_recap.PRC = (4*((OS)/2*10000)/12)+(15*((Pyriet)*10000)/120);

017_CEC_HL_gt20  UPDATE  basis_recap  SET  basis_recap.CEC  =  2.7*[lutum]+15.2*[OS]  WHERE  (((basis_recap.Formatie)="HL")  AND
((basis_recap.OS)>=20));

017_CEC_HL_sl20  UPDATE  basis_recap  SET  basis_recap.CEC  =  4*[lutum]+12.5*[OS]  WHERE  (((basis_recap.Formatie)="HL")  AND
((basis_recap.OS)<20));

017_CEC_PL       UPDATE basis_recap SET basis_recap.CEC = 5*[lutum]+15*[OS] WHERE (((basis_recap.Formatie)<>"HL"));

018_CPBO        UPDATE basis_recap SET basis_recap.CPBO = (((Carbonaat)/100)*10000)-(2*((Pyriet)/120)*10000);

20_reacCap      SELECT  basis_recap.Basis_ID  AS  ID,  basis_recap.[X  coordinaat],  basis_recap.[Y  coordinaat],  basis_recap.BORING,
basis_recap.FromTable,  basis_recap.Mid,  basis_recap.LocDepth_ID,  "NL"  AS  Subgebied,  basis_recap.ZKVFomatie,
basis_recap.ZKV_NEW  AS  LITH_NEW,  Null  AS  ZKV,  basis_recap.Formatie,  basis_recap.diepte,  basis_recap.Fe_reac,
basis_recap.Pyriet,  basis_recap.S_org,  basis_recap.S_gedegen,  basis_recap.lutum,  basis_recap.OS  AS  Org_stof,
basis_recap.Carbonaat, basis_recap.PRC, basis_recap.CEC, basis_recap.CPBO, 25 AS depth_class INTO New_analysis_recap FROM
basis_recap WHERE (((basis_recap.ZKV_NEW)<>"S") AND ((basis_recap.Formatie) Is Not Null And (basis_recap.Formatie) Not Like
"geen*") AND ((basis_recap.diepte)>25));

21_FmNotUsed    SELECT  New_analysis_recap.Formatie, Count(New_analysis_recap.ID) AS CountOfID, New_analysis_recap.depth_class AS Expr1
FROM New_analysis_recap GROUP BY New_analysis_recap.Formatie, New_analysis_recap.depth_class;

21_ge30         UPDATE New_analysis_recap SET New_analysis_recap.depth_class = 30 WHERE (((New_analysis_recap.diepte)>=30));

22_del_FmNotUsed DELETE New_analysis_recap.Formatie FROM New_analysis_recap WHERE (((New_analysis_recap.Formatie)="BE" Or
(New_analysis_recap.Formatie)="DO" Or (New_analysis_recap.Formatie)="DR" Or (New_analysis_recap.Formatie)="EE" Or
(New_analysis_recap.Formatie)="GU" Or (New_analysis_recap.Formatie)="HT" Or (New_analysis_recap.Formatie)="MT" Or
(New_analysis_recap.Formatie)="TO" Or (New_analysis_recap.Formatie)="HL"));

23_dataPerFm    SELECT  New_analysis_recap.Formatie, New_analysis_recap.depth_class, Count(New_analysis_recap.ID) AS CountOfID FROM
New_analysis_recap GROUP BY New_analysis_recap.Formatie, New_analysis_recap.depth_class ORDER BY
Count(New_analysis_recap.ID);

24_boring_pivot SELECT  Left([LocDepth_ID],6) AS BORING, New_analysis_recap.Formatie, New_analysis_recap.depth_class,
Count(New_analysis_recap.ID) AS CountOfID FROM New_analysis_recap GROUP BY Left([LocDepth_ID],6),
New_analysis_recap.Formatie, New_analysis_recap.depth_class HAVING (((New_analysis_recap.depth_class)=25)) ORDER BY
Count(New_analysis_recap.ID);

25_remove_25_1  DELETE  New_analysis_recap.depth_class,  New_analysis_recap.Formatie,  New_analysis_recap.LocDepth_ID  FROM
New_analysis_recap WHERE (((New_analysis_recap.depth_class)=25) AND ((New_analysis_recap.LocDepth_ID) Not Like "B30G08*"
And (New_analysis_recap.LocDepth_ID) Not Like "B31D01*" And (New_analysis_recap.LocDepth_ID) Not Like "B34C01*" And
(New_analysis_recap.LocDepth_ID) Not Like "B03G01*" And (New_analysis_recap.LocDepth_ID) Not Like "B11F01*" And
(New_analysis_recap.LocDepth_ID) Not Like "B12D00*" And (New_analysis_recap.LocDepth_ID) Not Like "B17G00*" And
(New_analysis_recap.LocDepth_ID) Not Like "B53F00*" And (New_analysis_recap.LocDepth_ID) Not Like "B54A00*" And
(New_analysis_recap.LocDepth_ID) Not Like "B54B00*" And (New_analysis_recap.LocDepth_ID) Not Like "B54E03*"));

25_remove_25_2  DELETE  New_analysis_recap.depth_class,  New_analysis_recap.Formatie  FROM  New_analysis_recap  WHERE
(((New_analysis_recap.depth_class)=25) AND ((New_analysis_recap.Formatie)<>"KR" And (New_analysis_recap.Formatie)<>"PE" And
(New_analysis_recap.Formatie)<>"RU"));

26_Sorg_Null    UPDATE  New_analysis_recap  SET  New_analysis_recap.S_org  =  Null  WHERE  (((New_analysis_recap.S_org)=0)  AND
((New_analysis_recap.Fe_reac) Is Null) AND ((New_analysis_recap.Pyriet) Is Null) AND ((New_analysis_recap.S_gedegen) Is Null) AND
((New_analysis_recap.lutum) Is Null) AND ((New_analysis_recap.Org_stof) Is Null) AND ((New_analysis_recap.Carbonaat) Is Null));

27_Clay         UPDATE New_analysis_recap SET New_analysis_recap.LITH_NEW = "C" WHERE (((New_analysis_recap.LITH_NEW)="K"));

27_Fluviatiel   UPDATE  New_analysis_recap  SET  New_analysis_recap.Subgebied  =  "Riverine"  WHERE  (((New_analysis_recap.Formatie)="AP"  Or
(New_analysis_recap.Formatie)="Kr"  Or  (New_analysis_recap.Formatie)="KI"  Or  (New_analysis_recap.Formatie)="URVE"  Or

```

```

(New_analysis_recap.Formatie)="URTY" Or (New_analysis_recap.Formatie)="SY" Or (New_analysis_recap.Formatie)="ST" Or
(New_analysis_recap.Formatie)="PZWA");

27_Marien UPDATE New_analysis_recap SET New_analysis_recap.Subgebied = "Marine" WHERE (((New_analysis_recap.Formatie)="RU" Or
(New_analysis_recap.Formatie)="N" Or (New_analysis_recap.Formatie)="BR" Or (New_analysis_recap.Formatie)="MS" Or
(New_analysis_recap.Formatie)="OO");

27_Peat UPDATE New_analysis_recap SET New_analysis_recap.LITH_NEW = "P" WHERE (((New_analysis_recap.LITH_NEW)="V");

27_RestFm UPDATE New_analysis_recap SET New_analysis_recap.Subgebied = "Other Formations" WHERE
(((New_analysis_recap.Subgebied)="NL");

27_Sand UPDATE New_analysis_recap SET New_analysis_recap.LITH_NEW = "S" WHERE (((New_analysis_recap.LITH_NEW)="Z");

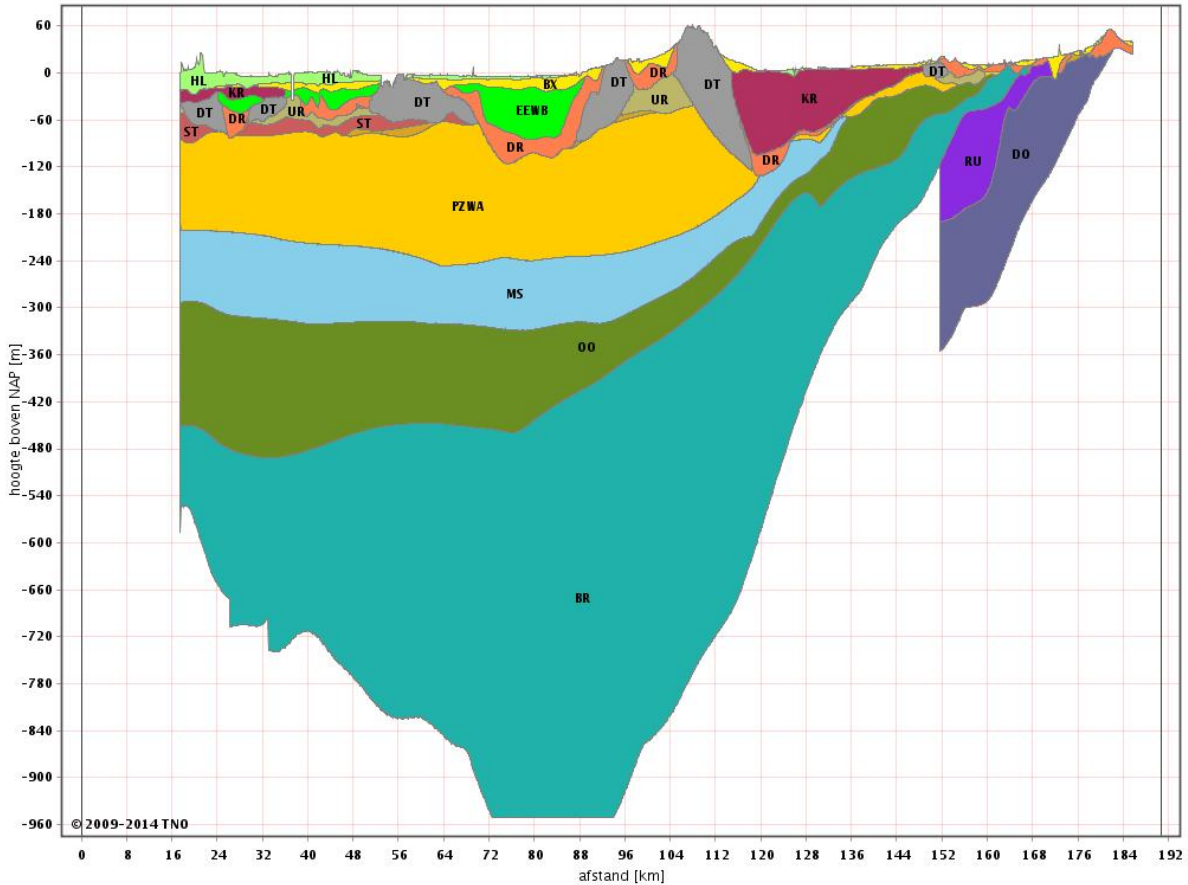
28_New_analysis_Recap_location SELECT New_analysis_recap.[X coördinaat], New_analysis_recap.[Y coördinaat], New_analysis_recap.BORING,
Count(New_analysis_recap.ID) AS CountOfID, Max(New_analysis_recap.diepte) AS MaxOfdiepte FROM New_analysis_recap GROUP
BY New_analysis_recap.[X coördinaat], New_analysis_recap.[Y coördinaat], New_analysis_recap.BORING;

29_ZKVFormatie UPDATE New_analysis_recap SET New_analysis_recap.ZKVFormatie = [LITH_NEW] & "-" & [Formatie];

30_reacCapExport SELECT New_analysis_recap.ID, New_analysis_recap.LocDepth_ID, New_analysis_recap.Subgebied,
New_analysis_recap.LITH_NEW, New_analysis_recap.ZKV, New_analysis_recap.Formatie, New_analysis_recap.diepte,
New_analysis_recap.Fe_reac AS Fe_reactive, New_analysis_recap.Pyriet AS Pyrite, New_analysis_recap.S_org AS S_organic,
New_analysis_recap.S_gedegen AS S_elemental, New_analysis_recap.lutum AS Clay_content, New_analysis_recap.Org_stof AS
Org_matter, New_analysis_recap.Carbonaat AS Carbonate, New_analysis_recap.PRC, New_analysis_recap.CEC,
New_analysis_recap.CPBO, New_analysis_recap.depth_class INTO New_analysis_recap_en FROM New_analysis_recap;

```

E Geological cross-sections

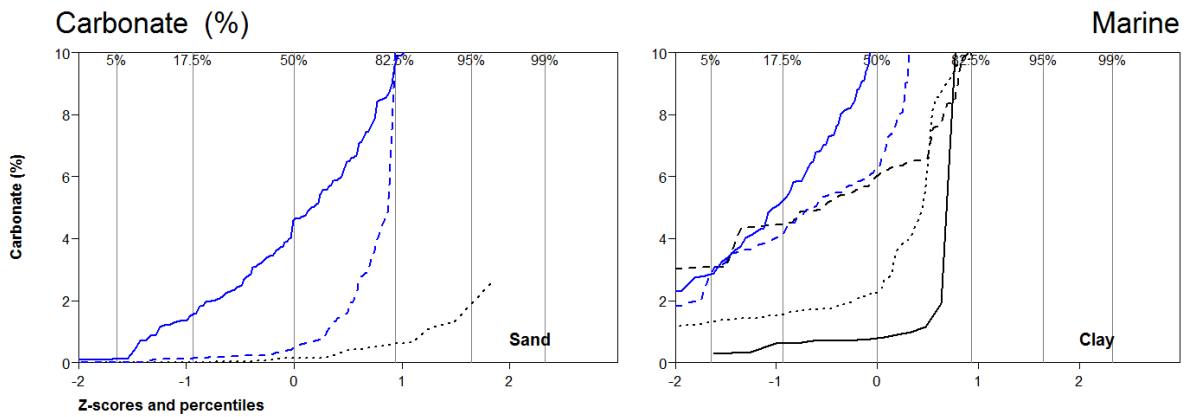


Landelijk model DGM v1.3 - 2009

- | | |
|------|------------------------------|
| HL | 01-Holocene afzettingen |
| BX | 02-Formatie van Boxtel |
| KR | 04-Formatie van Kreftenheye |
| EEWB | 05-Eem Formatie |
| DR | 07-Formatie van Drente |
| DT | 08-Gestuwde afzettingen |
| UR | 12-Formatie van Urk |
| ST | 13-Formatie van Sterksel |
| AP | 14-Formatie van Appelscha |
| PZWA | 16-Formatie van Peize-Waalre |
| MS | 17-Formatie van Maassluis |
| OO | 19-Formatie van Oosterhout |
| BR | 20-Formatie van Breda |
| RU | 21-Formatie van Rupel |
| DO | 23-Formatie van Dongen |

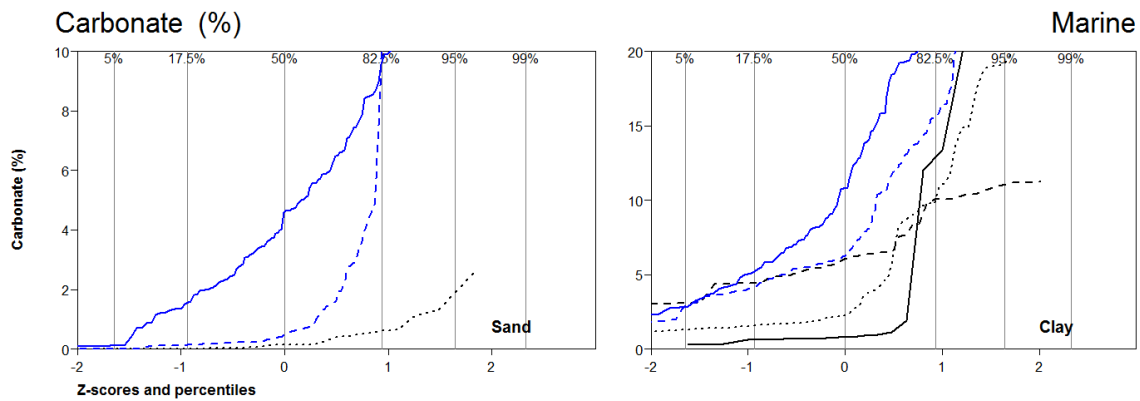
Geological east-west cross-section across the Netherlands following the line Haarlem (left) - Enschede (right) according to DGM v1.3 - 2009

F Statistics



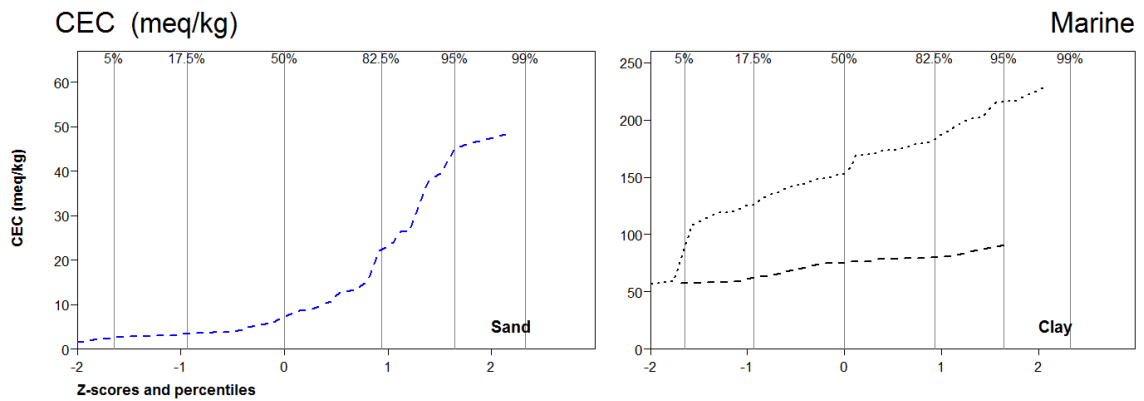
	n	p17.5	p50	p82.5	avg	std
Sand						
RU	7		0.4			
N	16	4	8.3	23.2	11.2	8
BR	30	0	0.1	0.6	0.4	0.7
MS	132	1.6	4.6	9.6	5.5	4.8
OO	161	0.1	0.4	10.2	5.8	12.4
Clay						
RU	20	0.6	0.8	12.9	24.3	65.1
N	46	4.4	6	10.1	6.6	2.4
BR	80	1.6	2.3	10	6.7	11.7
MS	115	5.2	10.8	21.4	13.2	8.7
OO	150	4.1	6.2	15.7	9.9	7.3

— RU
 - - - N
 BR
 — MS
 - - - OO



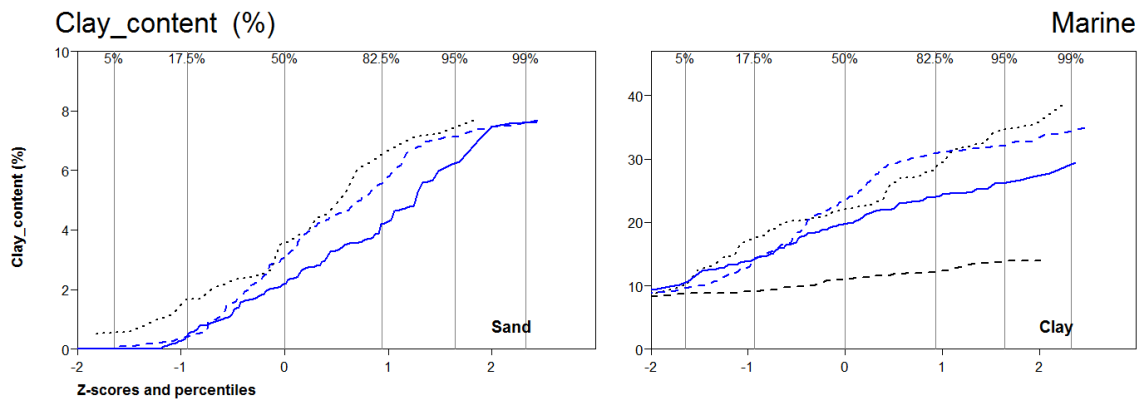
	n	p17.5	p50	p82.5	avg	std
Sand						
RU	7		0.4			
N	16	4	8.3	23.2	11.2	8
BR	30	0	0.1	0.6	0.4	0.7
MS	132	1.6	4.6	9.6	5.5	4.8
OO	161	0.1	0.4	10.2	5.8	12.4
Clay						
RU	20	0.6	0.8	12.9	24.3	65.1
N	46	4.4	6	10.1	6.6	2.4
BR	80	1.6	2.3	10	6.7	11.7
MS	115	5.2	10.8	21.4	13.2	8.7
OO	150	4.1	6.2	15.7	9.9	7.3

— RU
 - - - N
 BR
 — MS
 - - - OO



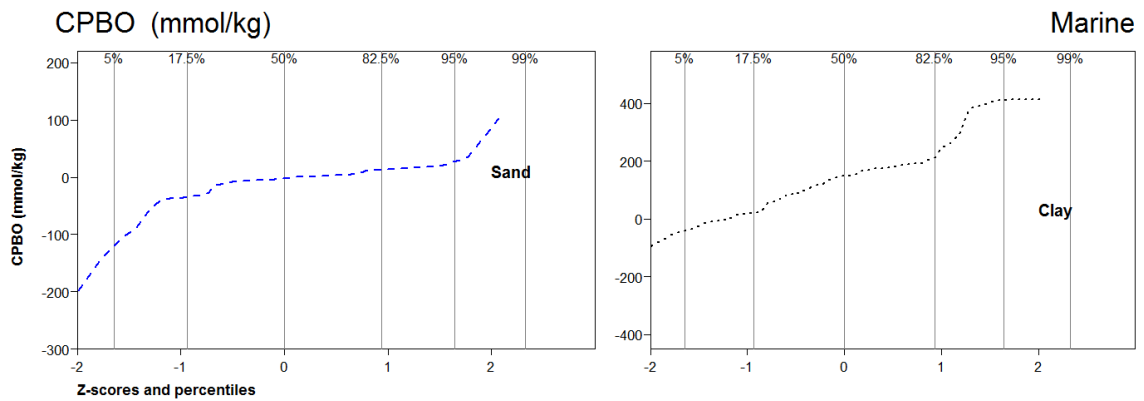
	n	p17.5	p50	p82.5	avg	std
Sand						
RU	7		28.9			
N	8	32.1	37.2	48.5	39.4	8.9
BR	9	5.8	23.7	26.7	21.2	19.7
MS	0					
OO	62	3.5	7.3	22.4	12.1	12.7
Clay						
RU	14	64.3	88.4	140.3	105.6	54.4
N	23	62.6	75.5	79.8	73.5	10.4
BR	52	125.7	153.6	183.3	156.2	38.9
MS	0					
OO	19	85.8	122.8	157	124.9	42.8

— RU
 - - - N
 BR
 MS
 - - - OO



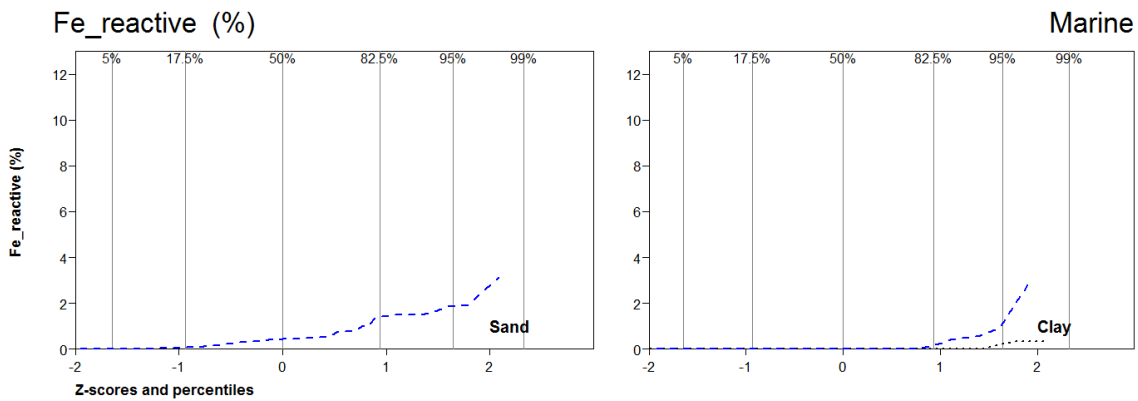
	n	p17.5	p50	p82.5	avg	std
Sand						
RU	7		5.5			
N	16	3.1	5.5	7.5	5.5	1.9
BR	30	1.7	3.6	6.5	3.7	2.3
MS	132	0.5	2.2	4.2	2.5	1.9
OO	161	0.4	3	5.6	3.2	2.3
Clay						
RU	18	10.6	13.7	18.9	16.2	8.4
N	46	9.1	11	12.2	10.9	1.6
BR	79	17.5	22.1	28.6	22.8	7.1
MS	115	14.2	19.7	24.1	19.4	4.9
OO	150	14.3	23.5	30.9	22.8	7.8

— RU
 - - - N
 BR
 — MS
 - - - OO



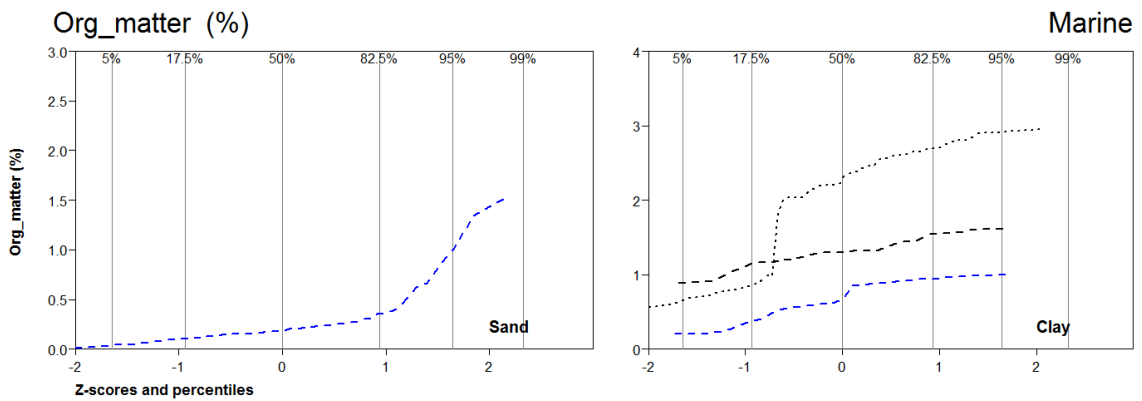
	n	p17.5	p50	p82.5	avg	std
Sand						
RU	4		5.3			
N	0					
BR	9	6.3	15.7	48.6	25.3	22.1
MS	0					
OO	53	-34.4	-2.4	13.7	-13.4	67.7
Clay						
RU	5		-20			
N	0					
BR	52	20.9	148.1	214.9	145.4	136.4
MS	0					
OO	19	-105.2	341.5	438.5	219.6	287.6

— RU
 - - - N
 BR
 — MS
 - - - OO



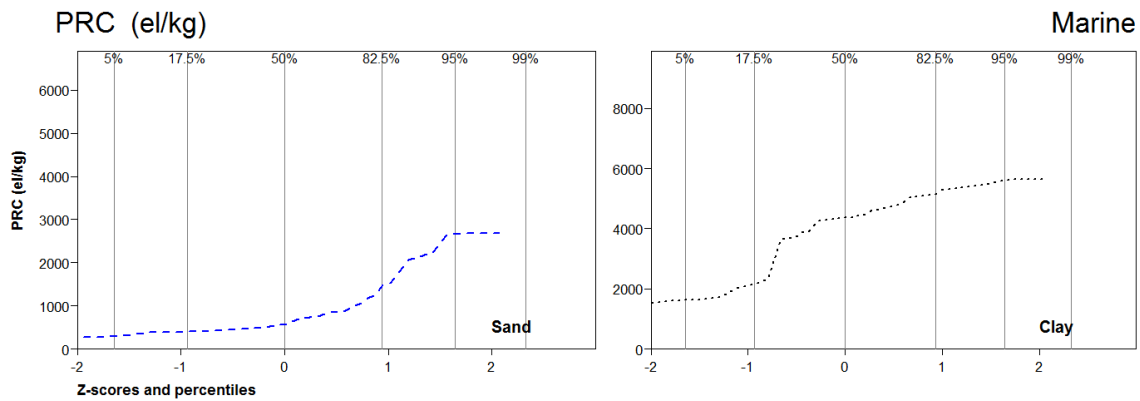
	n	p17.5	p50	p82.5	avg	std
Sand						
RU	4		1.8			
N	0					
BR	9	0.1	3.1	8.7	4.1	4.7
MS	0					
OO	55	0.1	0.4	1.4	0.7	1.1
Clay						
RU	7		1.1			
N	0					
BR	53	0	0	0	0	0.1
MS	3		0			
OO	38	0	0	0.2	0.2	0.8

— RU
 - - - N
 BR
 — MS
 - - - OO



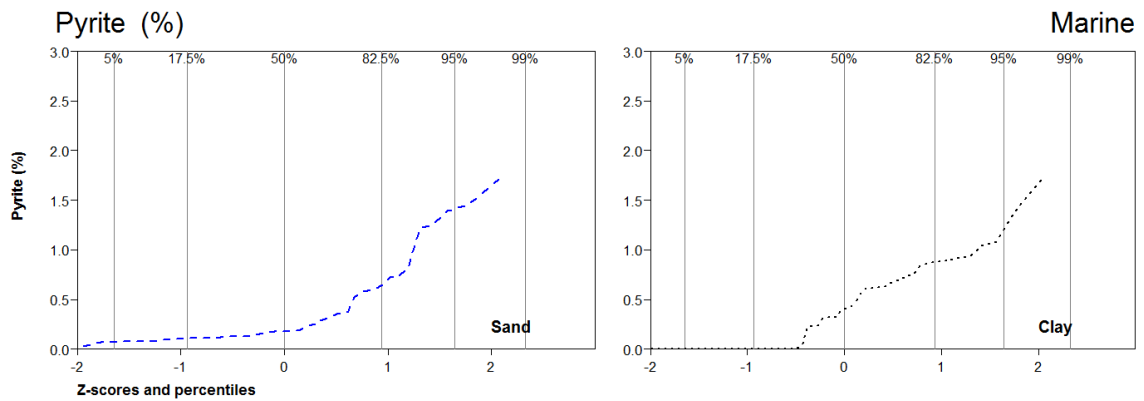
	n	p17.5	p50	p82.5	avg	std
Sand						
RU	7		0.3			
N	8	0.5	0.8	1.1	0.8	0.4
BR	9	0	0.1	0.4	0.3	0.7
MS	0					
OO	62	0.1	0.2	0.4	0.3	0.3
Clay						
RU	14	0.4	0.9	2	1.3	1.1
N	23	1.1	1.3	1.5	1.3	0.2
BR	52	0.9	2.3	2.7	2	0.8
MS	0					
OO	25	0.4	0.7	0.9	0.7	0.3

— RU
 - - - N
 BR
 — MS
 - - - OO



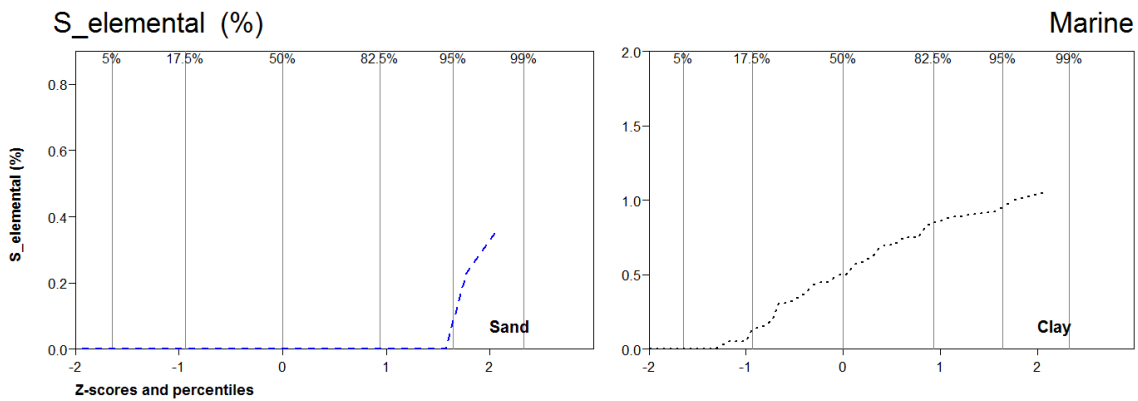
	n	p17.5	p50	p82.5	avg	std
Sand						
RU	4		642.7			
N	0					
BR	9	112.1	245.7	767	730.4	1270.3
MS	0					
OO	53	406.5	561.9	1466.7	966.5	1054.7
Clay						
RU	5		4369.2			
N	0					
BR	52	2154.6	4366.6	5158.3	4002.6	1320.9
MS	0					
OO	19	1628.9	2253.7	3552.8	2833.5	1927.7

— RU
 - - - N
 BR
 — MS
 - - - OO



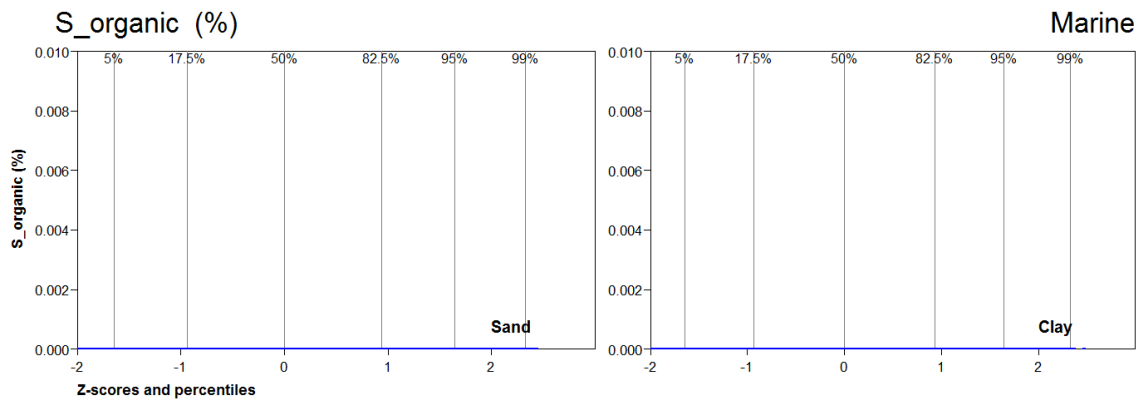
	n	p17.5	p50	p82.5	avg	std
Sand						
RU	4		0.5			
N	0					
BR	9	0	0	0.2	0.1	0.2
MS	0					
OO	53	0.1	0.2	0.6	0.4	0.5
Clay						
RU	5		0.6			
N	0					
BR	52	0	0.4	0.9	0.5	0.5
MS	0					
OO	19	0	0.8	2.1	1.2	1.6

— RU
 - - - N
 BR
 — MS
 - - - OO



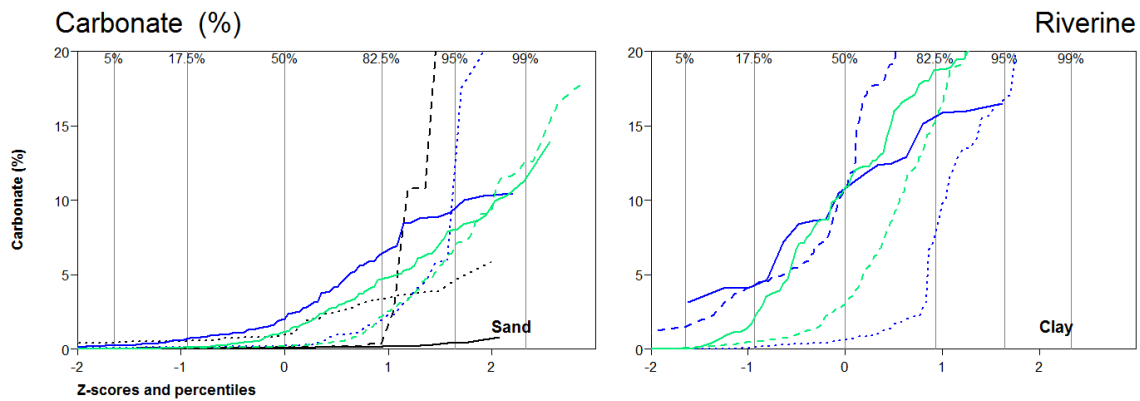
	n	p17.5	p50	p82.5	avg	std
Sand						
RU	4		0			
N	0					
BR	9	0	0	0	0	0
MS	0					
OO	53	0	0	0	0	0.1
Clay						
RU	5		0			
N	0					
BR	52	0.1	0.5	0.9	0.5	0.3
MS	0					
OO	19	0	0.3	0.8	0.3	0.4

— RU
 - - - N
 BR
 — MS
 - - - OO



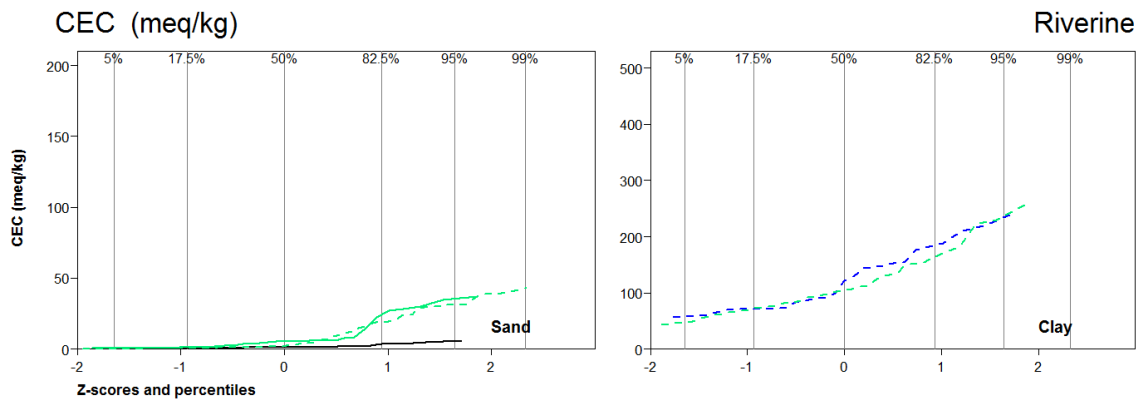
	n	p17.5	p50	p82.5	avg	std
Sand						
RU	7		0			
N	16	0	0	0	0	0
BR	30	0	0	0	0	0
MS	132	0	0	0	0	0
OO	161	0	0	0	0	0
Clay						
RU	20	0	0	0	0	0
N	46	0	0	0	0	0
BR	80	0	0	0	0	0
MS	115	0	0	0	0	0
OO	156	0	0	0	0	0

— RU
 - - - N
 . . . BR
 — MS
 - - - OO

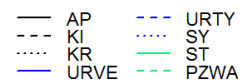


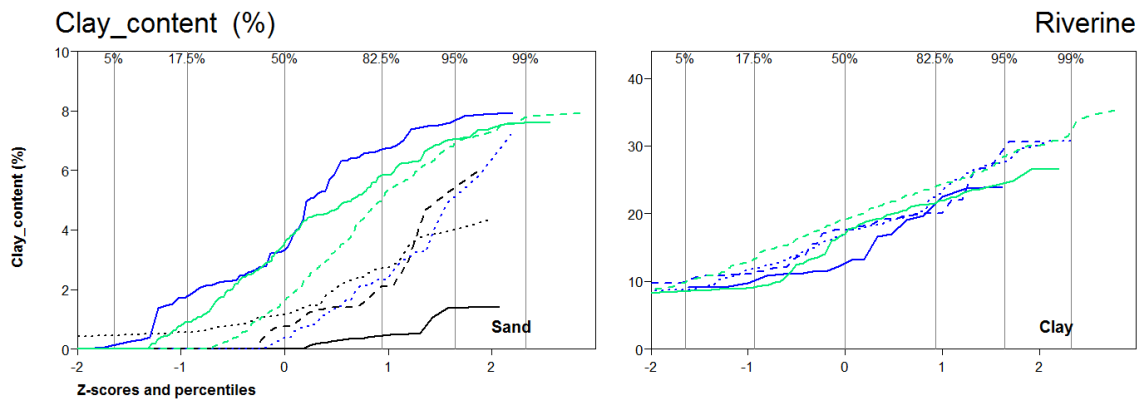
	n	p17.5	p50	p82.5	avg	std
Sand						
AP	53	0.1	0.1	0.2	0.1	0.2
KI	35	0	0.1	0.5	7.1	27
KR	44	0.5	1	3.3	2	2
URVE	73	0.7	2	6.4	3.5	3.8
URTY	16	1	4.4	15.4	7.9	8.8
SY	70	0.1	0.2	2	2.1	5.5
ST	191	0.1	1.1	4.7	2.3	2.8
PZWA	483	0	0.2	2.2	1.3	2.7
Clay						
AP	1		2.1			
KI	19	0	1.3	110	40.6	60.1
KR	8	0.2	0.4	3.3	2.1	3.6
URVE	20	4.3	10.8	15.6	10.1	5
URTY	103	4.3	10.7	27.5	17.3	17.3
SY	115	0.1	0.6	7.7	3.5	6.2
ST	73	2.1	10.8	18.8	11	7.7
PZWA	366	0.5	3	15.4	7	8.2





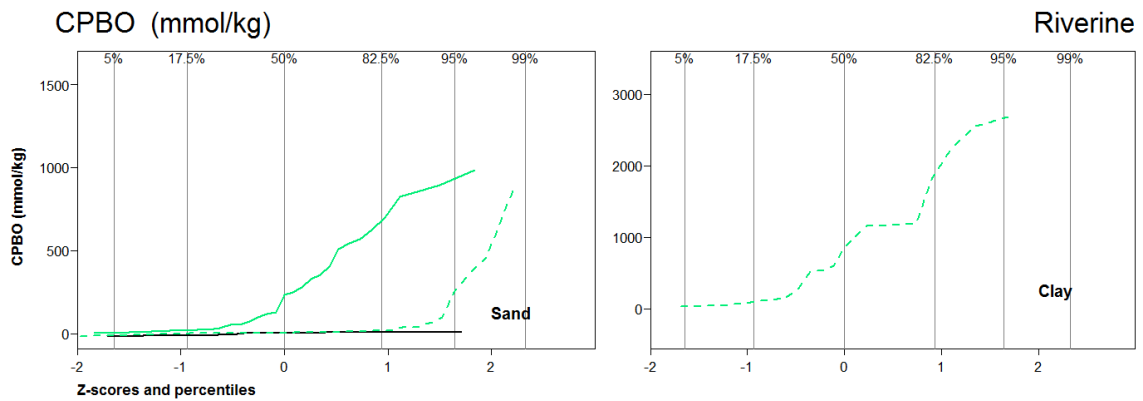
	n	p17.5	p50	p82.5	avg	std
Sand						
AP	24	0.9	1.3	3.4	2.2	2.6
KI	3		1.3			
KR	4		4.2			
URVE	4		8.3			
URTY	8	6.5	20.8	38.8	23	17.8
SY	1		5.1			
ST	33	1.1	5.3	24.4	15	36.3
PZWA	102	0.8	2.3	19.1	8.5	11.2
Clay						
AP	1		75.7			
KI	3		266.9			
KR	0					
URVE	0					
URTY	27	71.1	122.1	185.1	128.7	62.1
SY	16	98.2	135.2	174.9	148.9	72.3
ST	14	74.7	108.5	123.6	101.8	27.6
PZWA	35	71.9	103.5	164.4	126.9	86.6





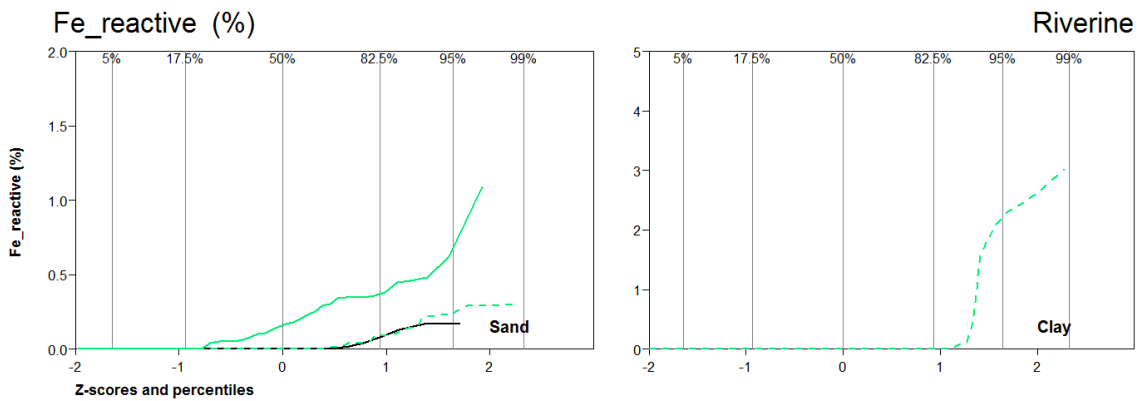
	n	p17.5	p50	p82.5	avg	std
Sand						
AP	53	0	0	0.4	0.3	0.5
KI	35	0	0.8	2.1	1.3	1.8
KR	45	0.6	1.2	2.7	1.7	1.4
URVE	73	1.8	3.3	6.7	4	2.5
URTY	16	0.6	1.6	5.8	2.9	2.5
SY	70	0	0.4	2.3	1.2	1.8
ST	191	0.9	3.6	5.8	3.4	2.2
PZWA	483	0	1.6	5	2.3	2.3
Clay						
AP	1		12.3			
KI	11	16.5	30.2	38	27.7	11.3
KR	8	8.7	11.2	25.3	16.7	12.8
URVE	20	10.1	12.7	21.5	15.4	6.6
URTY	45	11.3	17.6	20.1	17.4	5.8
SY	115	11.9	17.6	22.6	17.3	5.7
ST	73	9.1	17	21.6	16.2	5.7
PZWA	366	13.3	19.2	23.9	19	5.6





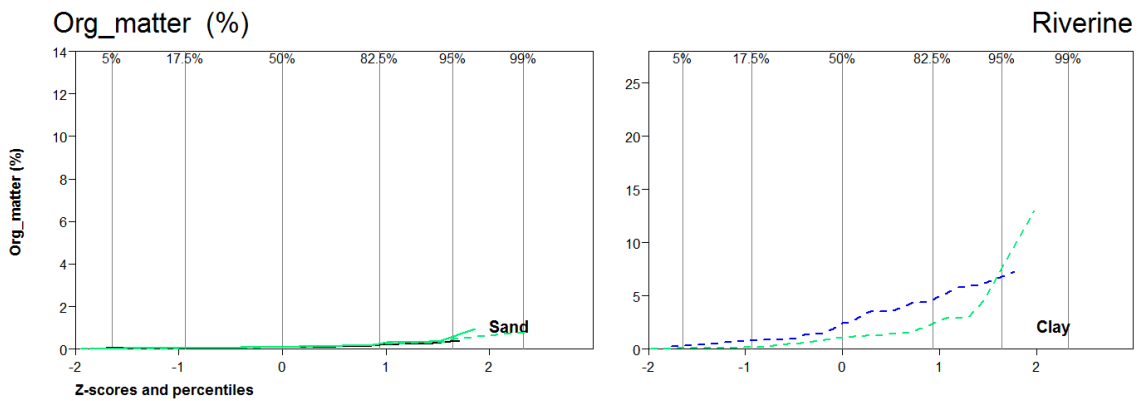
	n	p17.5	p50	p82.5	avg	std
Sand						
AP	24	-11.3	5.7	8.4	0.7	9.2
KI	2		7.7			
KR	4		48.3			
URVE	1		21.5			
URTY	0					
SY	1		139.2			
ST	31	21.3	232.9	681.2	324.6	345.5
PZWA	79	1.8	6.2	18.1	54	215.9
Clay						
AP	1		-85.8			
KI	3		127			
KR	0					
URVE	0					
URTY	0					
SY	16	-89.4	-36.2	25.4	-50.2	169.9
ST	14	1202.2	1705.6	1854.9	1604.6	606.4
PZWA	23	102.1	861.4	1889.9	1003.2	987

— AP - - - URTY
 - - - KI ····· SY
 ····· KR — ST
 — URVE - - - PZWA

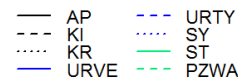


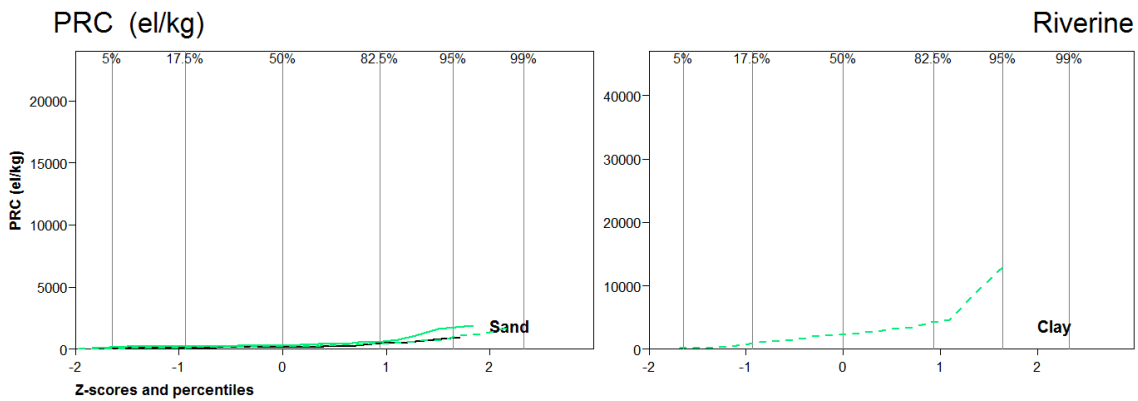
	n	p17.5	p50	p82.5	avg	std
Sand						
AP	24	0	0	0.1	0	0.1
KI	5		0			
KR	4		0			
URVE	2		0.1			
URTY	0					
SY	3		0			
ST	38	0	0.2	0.4	0.3	0.4
PZWA	81	0	0	0.1	0	0.1
Clay						
AP	1		1.7			
KI	13	0	0	0	0	0
KR	1		0			
URVE	0					
URTY	0					
SY	19	0	0.4	1.1	0.6	0.8
ST	14	1.2	1.7	2.5	2	1.2
PZWA	90	0	0	0	0.2	0.7

— AP - - - URTY
 - - - KI ····· SY
 ····· KR — ST
 — URVE - - - PZWA



	n	p17.5	p50	p82.5	avg	std
Sand						
AP	24	0.1	0.1	0.2	0.1	0.2
KI	3		0.1			
KR	4		0			
URVE	4		0.1			
URTY	8	0.2	0.3	0.5	0.5	0.6
SY	1		0.1			
ST	33	0	0.1	0.2	0.5	2.3
PZWA	102	0	0.1	0.2	0.1	0.2
Clay						
AP	1		1			
KI	4		2.9			
KR	0					
URVE	10	0	0.4	1.6	0.7	0.8
URTY	27	0.8	2.4	4.7	3	2.8
SY	16	0.4	0.8	5.4	3.3	4.8
ST	16	0.6	0.9	1.3	1	0.6
PZWA	43	0.2	1.1	2.4	2.2	4.6

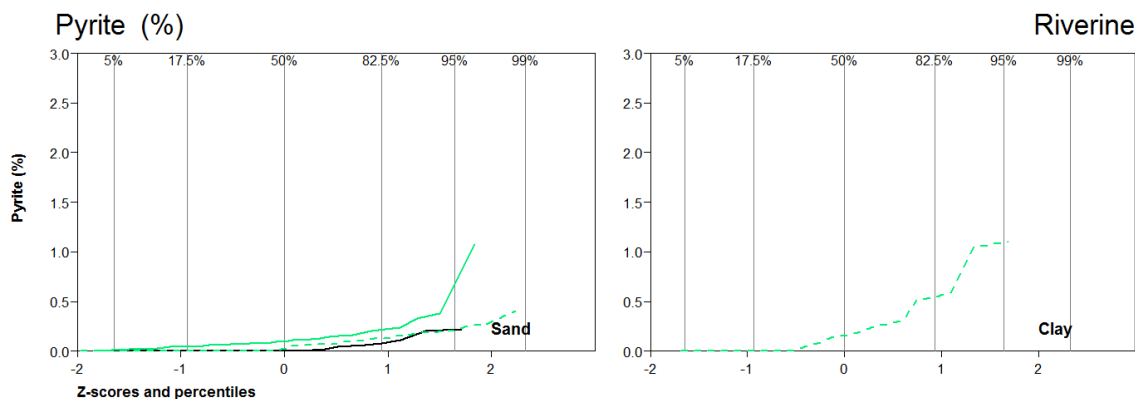




Z-scores and percentiles

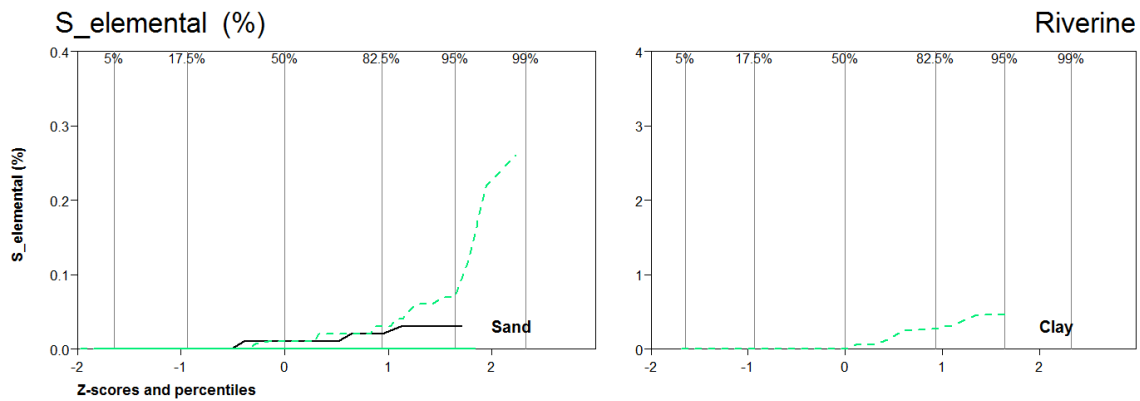
	n	p17.5	p50	p82.5	avg	std
Sand						
AP	24	109.1	155	479	295.2	347.7
KI	2		139.4			
KR	4		176.8			
URVE	1		1			
URTY	0					
SY	1		806.5			
ST	31	219.5	309.5	627	1191.1	4157.8
PZWA	79	102.4	195.6	430.6	324.5	420.8
Clay						
AP	1		3834.1			
KI	3		8631			
KR	0					
URVE	0					
URTY	0					
SY	16	855.6	1569.2	10149.3	6442.1	9541.2
ST	14	1351.9	1721.5	2502.2	2092.5	1006.9
PZWA	23	913.5	2233.9	4250.9	4757	9559.7

— AP - - - URTY
 - - - KI ····· SY
 ····· KR - - - ST
 - - - URVE - - - PZWA



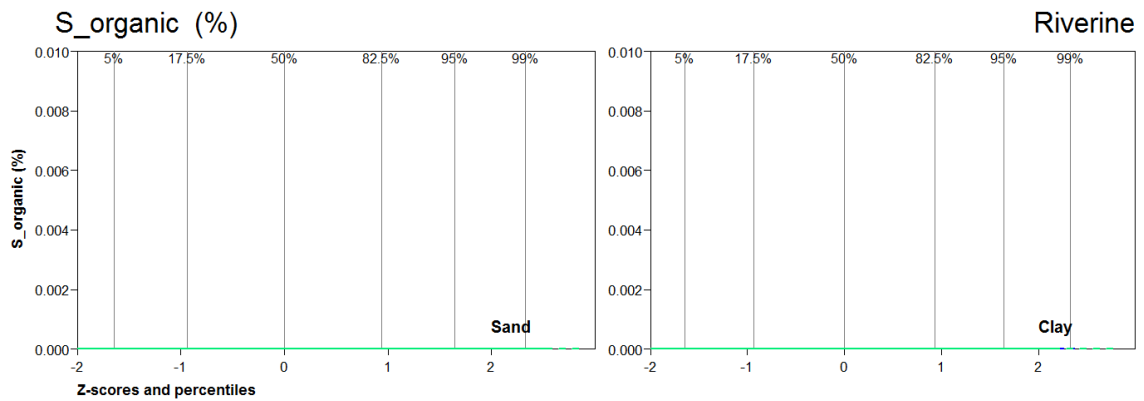
	n	p17.5	p50	p82.5	avg	std
Sand						
AP	24	0	0	0.1	0	0.1
KI	2		0			
KR	4		0.1			
URVE	1		0			
URTY	0					
SY	1		0.5			
ST	31	0	0.1	0.2	0.2	0.3
PZWA	79	0	0	0.1	0.1	0.1
Clay						
AP	1		1.8			
KI	3		0			
KR	0					
URVE	0					
URTY	0					
SY	16	0.1	0.3	1	0.8	1.2
ST	14	0.1	0.2	0.3	0.3	0.2
PZWA	23	0	0.2	0.5	0.3	0.4

— AP - - - URTY
 - - - KI ····· SY
 ····· KR — ST
 — URVE - - - PZWA



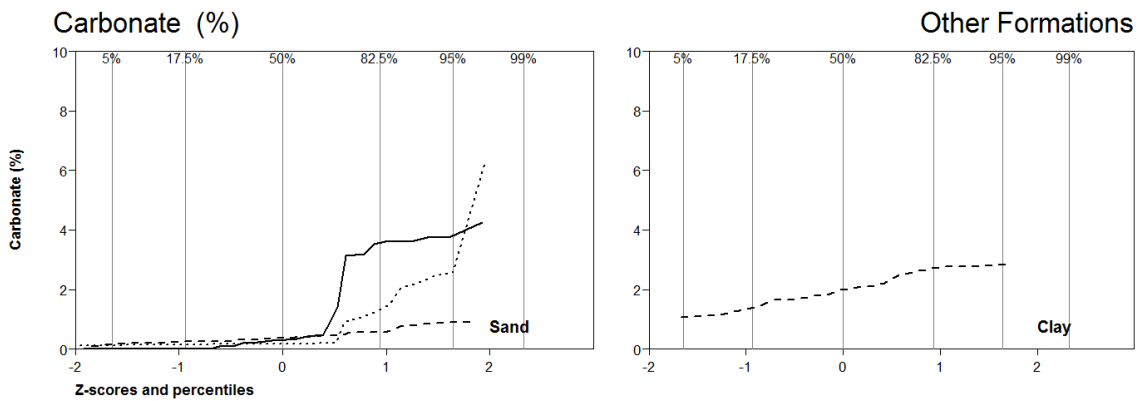
	n	p17.5	p50	p82.5	avg	std
Sand						
AP	24	0	0	0	0	0
KI	2		0			
KR	4		0			
URVE	1		0			
URTY	0					
SY	1		0.2			
ST	31	0	0	0	0	0
PZWA	79	0	0	0	0	0.1
Clay						
AP	1		0			
KI	3		0.2			
KR	0					
URVE	0					
URTY	0					
SY	16	0	0	0	0.1	0.4
ST	14	0	0	0	0	0
PZWA	23	0	0	0.3	0.2	0.6

— AP - - - URTY
 - - - KI ····· SY
 ····· KR - - - ST
 - - - URVE - - - PZWA



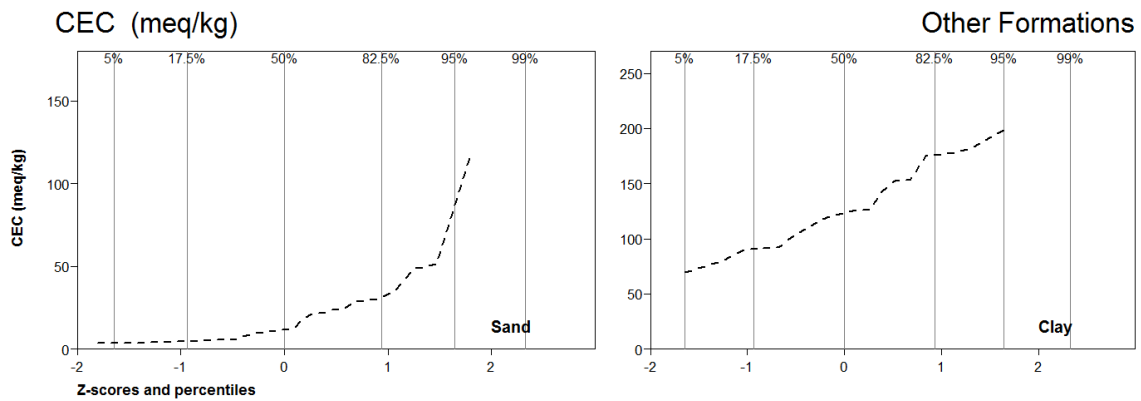
	n	p17.5	p50	p82.5	avg	std
Sand						
AP	53	0	0	0	0	0
KI	35	0	0	0	0	0
KR	45	0	0	0	0	0
URVE	73	0	0	0	0	0
URTY	16	0	0	0	0	0
SY	70	0	0	0	0	0
ST	191	0	0	0	0	0
PZWA	483	0	0	0	0	0
Clay						
AP	1		0			
KI	20	0	0	0	0	0
KR	8	0	0	0	0	0
URVE	30	0	0	0	0	0
URTY	103	0	0	0	0	0
SY	115	0	0	0	0	0
ST	75	0	0	0	0	0
PZWA	374	0	0	0	0	0

— AP - - - URTY
 - - - KI ····· SY
 ····· KR — ST
 — URVE - - - PZWA



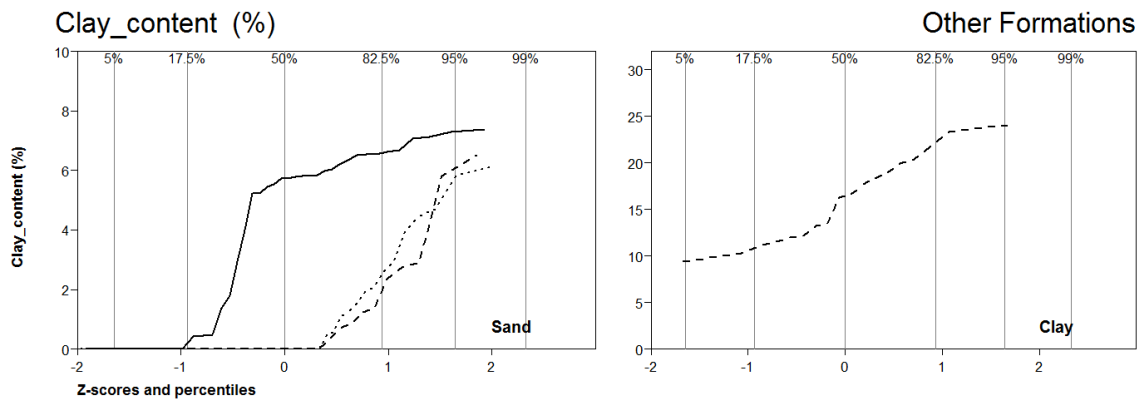
	n	p17.5	p50	p82.5	avg	std
Sand						
PE	38	0	0.3	3.6	1.3	1.7
BX	32	0.2	0.4	0.6	0.9	2.9
DT	41	0.2	0.2	1.3	0.8	1.5
Clay						
PE	13	0	7	10.2	5.8	4.6
BX	22	1.4	2	2.7	2	0.7
DT	14	4.7	10.4	16.1	10.2	6.1

— PE
 --- BX
 DT



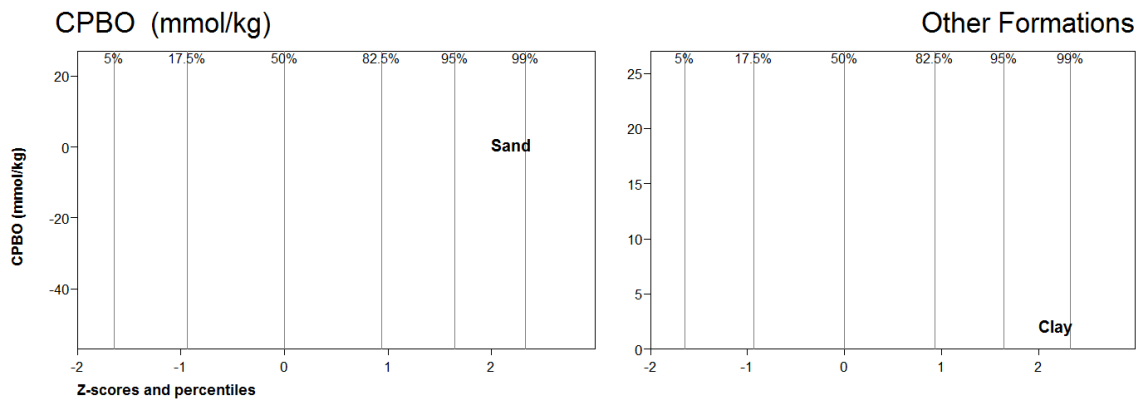
	n	p17.5	p50	p82.5	avg	std
Sand						
PE	16	1	3.4	35.5	15.4	21.7
BX	29	4.5	11.8	31	25.3	36.6
DT	0					
Clay						
PE	7		189.3			
BX	21	90.8	122.9	176	130.9	48.1
DT	0					

— PE
 - - - BX
 DT



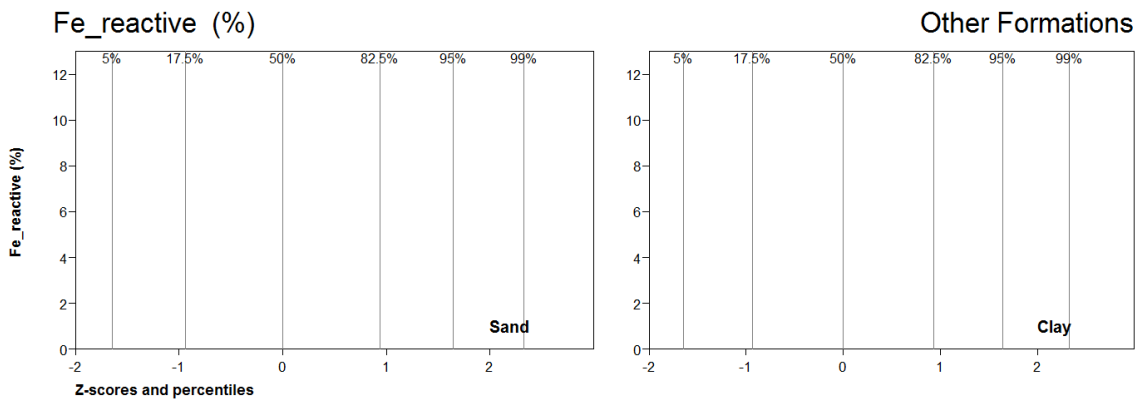
	n	p17.5	p50	p82.5	avg	std
Sand						
PE	38	0.2	5.7	6.6	4.2	2.8
BX	32	0	0	1.9	1	2
DT	42	0	0	2.5	1.1	1.9
Clay						
PE	13	9.8	21	28.7	20.4	8.5
BX	22	10.8	16.5	22.2	16.2	5.4
DT	14	11.9	16.8	21.5	17.4	5.8

— PE
 - - - BX
 DT



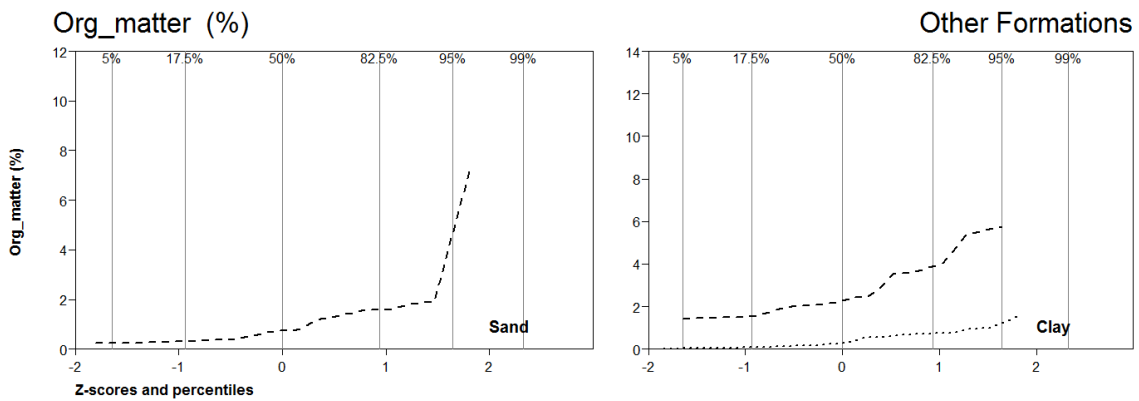
	n	p17.5	p50	p82.5	avg	std
Sand						
PE	16	-6.5	5.4	16.6	2.2	19.6
BX	0					
DT	0					
Clay						
PE	7		520.4			
BX	0					
DT	0					

— PE
 --- BX
 DT



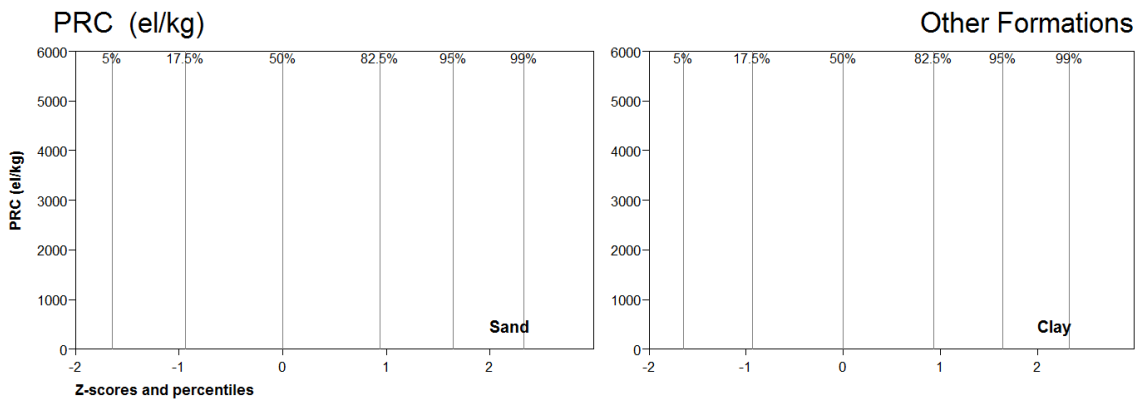
	n	p17.5	p50	p82.5	avg	std
Sand						
PE	16	0.1	0.2	1	1.2	3.1
BX	2		0			
DT	10	0	0	0	0	0
Clay						
PE	7		1.8			
BX	7		0			
DT	1		0			

— PE
- - - BX
..... DT



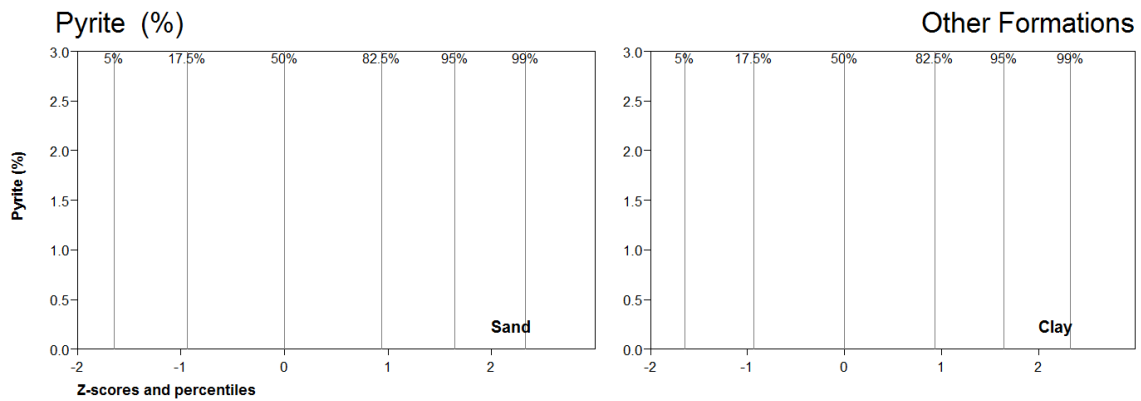
	n	p17.5	p50	p82.5	avg	std
Sand						
PE	16	0	0.2	0.9	0.6	0.8
BX	29	0.3	0.8	1.6	1.4	2.3
DT	0					
Clay						
PE	9	1.6	2.5	3.4	2.6	1.5
BX	21	1.6	2.3	3.9	3.2	2.8
DT	32	0.1	0.3	0.7	0.5	0.6

— PE
 - - - BX
 DT



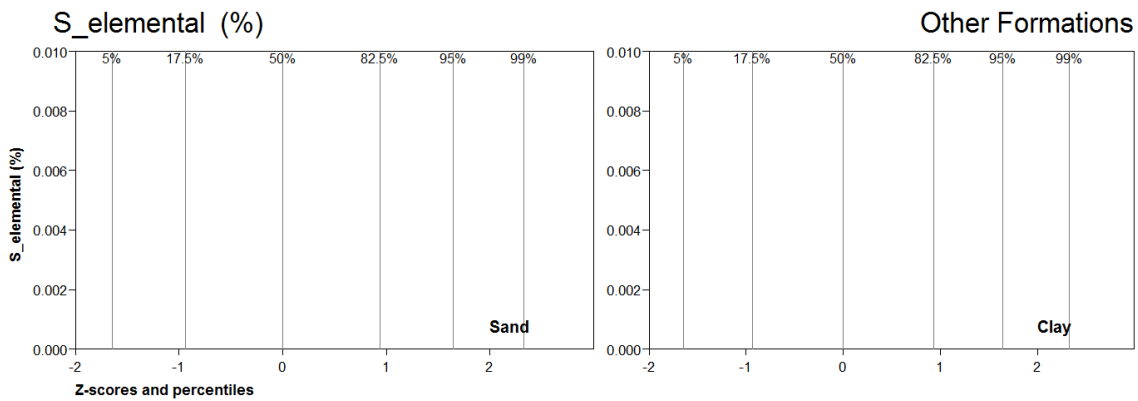
	n	p17.5	p50	p82.5	avg	std
Sand						
PE	16	168.1	390.2	2126.1	1196.7	1671.8
BX	0					
DT	0					
Clay						
PE	7		8315.4			
BX	0					
DT	0					

— PE
 - - - BX
 DT



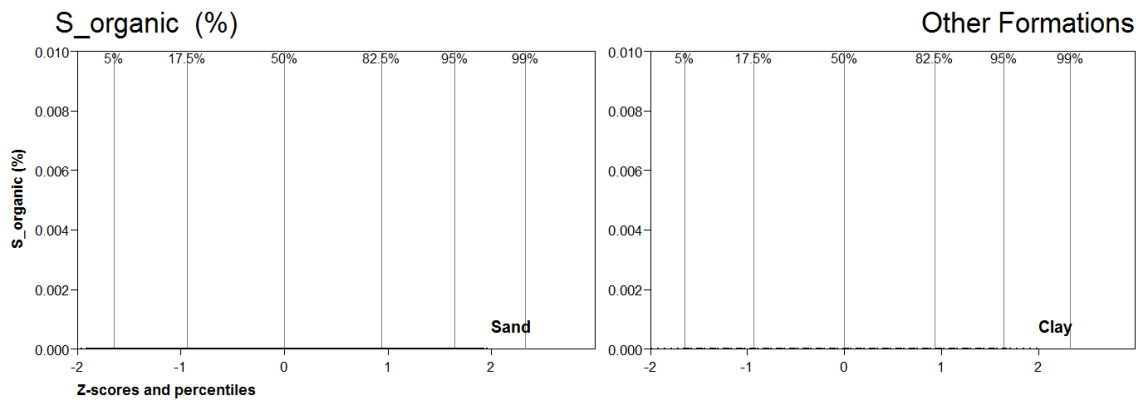
	n	p17.5	p50	p82.5	avg	std
Sand						
PE	16	0	0.1	0.3	0.2	0.3
BX	0					
DT	0					
Clay						
PE	7		2.4			
BX	0					
DT	0					

— PE
 --- BX
 DT



	n	p17.5	p50	p82.5	avg	std
Sand						
PE	16	0	0	0	0	0
BX	0					
DT	0					
Clay						
PE	7		0			
BX	0					
DT	0					

— PE
 --- BX
 DT



	n	p17.5	p50	p82.5	avg	std
Sand						
PE	38	0	0	0	0	0
BX	32	0	0	0	0	0
DT	42	0	0	0	0	0
Clay						
PE	15	0	0	0	0	0
BX	22	0	0	0	0	0
DT	46	0	0	0	0	0

— PE
 - - - BX
 DT